

Dear editor,

We are glad to submit our final response letter together with our revised manuscript to AMT.

In this document, we have included the mark-up version, and the response letter to all three reviewers. Please note that reviewer#2 has given a full review in the quick-review phase, and we have provided a corresponding revision. The current revision is mostly to address the comments from other two reviewers. Please note that the mark-up file indicates all changes since our first submission based on the comments and suggestions of all three reviewers.

Thank you and best wishes,

Meng

Response to the report of reviewer #1:

We appreciate the detailed comments and suggestions from the reviewer, which are very helpful in improving the clarity of this work. Please find our response as follows. We have made corresponding revisions in the manuscript also detailed below.

Interactive comment on “Inversion of multi-angular polarimetric measurements from the ACEPOL campaign: an application of improving aerosol property and hyperspectral ocean color retrievals” by Meng Gao et al.

Anonymous Referee #1 Received and published: 7 April 2020

The paper uses data collected from two airborne multi-angle polarimeters (MAPs) flying together on the ER-2 over a SeaPRISM site off the southern California coast to investigate whether multi-angle polarimetry will improve atmospheric correction of a hyperspectral instrument. The question is important because of the NASA PACE mission scheduled to launch in less than three years. The flagship PACE instrument is a hyperspectral radiometer, but it will be flying with two MAPs. Will those MAPs improve the radiometer’s ability to retrieve ocean-leaving radiance by constraining aerosol properties? The study is presented well, is backed up with real validation and comes to a solid conclusion. There are a few points that I think should be considered before publication, but overall my take is that the revisions will be very minor.

Thanks for the interest in this work and the positive comments.

Comments:

1. Addressing the lack of UV in the study.

For me the biggest challenge for atmospheric correction in PACE is not the hyperspectral, but the UV. The atmosphere in the UV range is thick with Rayleigh and with aerosol scattering/absorption, making atmospheric correction even more uncertain than it is even in the deep blue (410 nm). Yet, the ocean community is excited by the UV measurements by OCI and intends to exploit that data, which they absolutely will not be able to do without a better plan for UV atmospheric correction.

I fully understand that addressing UV is outside the scope of this paper, but there are small things that can be done here to clarify the limitations of this paper and express the need for a future focus on the UV. The authors would be doing the community a great service.

Thank you for the comments. We agree that the UV coverage which will be provided by PACE is important for both atmosphere and ocean community, but unfortunately it cannot be explored in this study due to the limitation in the measurement data. We have made necessary revisions to emphasize the importance of atmospheric correct at UV, which are listed below in the responses to the specific comments.

P3 Line 1. SPEXone has true UV measurements.

P4 Line 27. SPEX airborne does not have UV measurements

P3 Lines 21-22. “SPEX Airborne collects hyperspectral radiometry, and thus can be used as a proxy for OCI in developing hyperspectral ocean color algorithms.” With the

caveat that it is missing measurements in the true UV part of the range.

We added the following sentence to clarify the missing UV measurements in SPEX Airborne:

“The spectral range from the SPEX Airborne measurements used in this study is from 470 to 750 nm. This does not cover the UV bands, which is nevertheless important and deems further research for the PACE mission (Frouin et al 2019, Chowdhary et al 2019).”

P20 Line 2. “The resulting hyperspectral water leaving reflectances agree well with the AERONET OC and MODIS OC products.” But not below 470 nm. This has implications for the UV.

We revised the statement by specifying more details for both RSP Rrs and SPEX Rrs:

“...
The retrieval uncertainties on RSP Rrs is within 0.0004 sr^{-1} (same to SPEX Rrs), while the comparison of the two cases with the AERONET Rrs shows a difference less than 0.0003 sr^{-1} for RSP Rrs, and a maximum difference of 0.0004 sr^{-1} (Case 10/25) and 0.001 sr^{-1} (Case 10/23) for SPEX Rrs. The difference of SPEX Rrs for Case 10/23 is larger than the retrieval uncertainties which is likely due to the radiometric uncertainties from the sensors.

“

2. Cases at very low aerosol loading

The two cases examined in the study are at very low AOD. There are a few places in the paper where the low aerosol loading introduces some concerns. P5 Line 11. “For AOD less than 0.2, uncertainties in the AERONET inversion properties.... (Dubovik et al., 2000)”.

For what wavelength is $\text{AOD} < 0.2$?

Dubovik 2000 is a very old reference. I looked through the materials on the AERONET web site including this document.

https://aeronet.gsfc.nasa.gov/new_web/Documents/U27_summary_final.pdf

It seems to imply a different set of uncertainties that are actually larger than what is stated here, especially for refractive indices and SSA. Size distribution products can tolerate lower aerosol loading, but anything to do with absorption just falls apart when there is insufficient signal.

Also the implication by this statement on P5 is that the same uncertainties hold for all AOD 0.2 and less. This means that $\text{AOD} = 0.04$ has the same uncertainties as $\text{AOD} = 0.20$, and the AERONET document, and especially the graphs at the bottom do not support this.

Now I find it interesting that the authors do mention the challenge of retrieving microphysical properties when the aerosol loading is small. (P6 Line 15 and P16 Lines 6-8).

Then why imply minimal uncertainty for these very, very low loadings of the cases studied in this paper? I am sufficiently distressed about trying to make retrievals of intrinsic particle properties when the AOD at 550 nm is less than 0.04, that I question the results of these retrievals in Figure 5 and Table 3, and some of the overall conclusions.

Thank you for the comments on the AOD, also thank you for providing the AERONET uncertainty document. We agree that the statement on the AERONET aerosol uncertainties may not best describe the particular cases in our study. We revised our manuscript according to the reviewer's suggestions, which are listed below in the responses of specific comments.

Specific items that need to be addressed:

The statement on P5 should be updated.

It is challenging to provide an accurate theoretical assessment of the uncertainties for the particular cases in our studies, we removed the general statement, and instead we only use the uncertainties evaluated by the daily average of the AERONET product as an estimate. We also made it explicit that the inversion uncertainties increase with smaller AOD by citing the AERONET uncertainty document:

“Note that the actual inversion uncertainties for the aerosol properties, such as the refractive index and single scattering albedo (SSA), may be larger than their daily averaged result for small AOD cases as reported by the AERONET Version 3 uncertainty analysis (Description of Aerosol Inversion Uncertainty for Level 2 Products). In general, AERONET retrievals of aerosol microphysical properties become less certain as AOD decreases.”

In figure 5, the AERONET properties are plotted with their daily variation, but not their uncertainties. The uncertainties are larger than the range of the daily variation. This should be stated explicitly.

We specifically mentioned that the AERONET results are plotted with its daily variation as:

“The results from AERONET product are plotted in green, and the vertical width indicates its daily variation.”

The possible larger uncertainty from AERONET product are also added as in the response to the last comment.

P16 Line 4, check those AERONET uncertainties again. I think they are too small.

This is similar to the above statement in P5, we removed it.

P19 Line 16. The absolute values also agree better with the AERONET aerosol product. “ This is not true for SSA. But... there are large uncertainties for SSA in AERONET because of the low AOD.

We revised it as follows:

“The absolute values also agree better with the AERONET aerosol product except SSA probably due to the large uncertainty of SSA from both the MAP and AERONET inversions at low AOD.”

3. Systematic biases between airborne SPEX and RSP

Beginning on P6 Line 28, the paper mentions “systematic differences”, but never describes which is higher, SPEX or RSP. This becomes important in the conclusion. P17

Lines 15-18. Here systematic differences between RSP and SPEXairborne are mentioned again, but which one is higher? And it isn’t stated which one is right. So when speaking of impact on aerosol retrievals, how would these instrumental differences cascade into the aerosol retrievals? What should be expected from these differences, and why or why not were these expectations met?

Thank you for the questions. The systematic differences the reviewer referred are the differences in radiometric calibration between the two instruments as reported by Smit et al 2019. The radiometric bias from both instruments could contribute to the systematic difference between these two instruments. We have revised the paragraph to indicate which sensor has larger reflectance as follows:

“...Over the four RSP bands of 410, 470, 550, 670 nm, the random noise contribution to differences of reflectance are 2%, 2%, 2% and 4%. RSP reflectance is slightly larger than SPEX reflectance at 410 and 470 nm as indicated by their systematic differences of around 4% and 3% respectively, larger than the random differences; the systematic differences at the other two bands are relatively small with values of 0% and 1%.”

From the comparison of the Rrs with AERONET Rrs, it seems the radiometric calibration of RSP is more accurate at 410 and 470 nm (as in the revised statement in the response of comment 1). But it is not our intention to claim which measurement is more accurate than the other based on only two case studies. Moreover, in terms of aerosol retrievals, we are trying to mitigate the issues by relying more on the RSP DoLP measurements which has smaller systematic difference between instrument and also high sensor accuracy.

P17 Lines 21-23. Once again we are presented with differences, but are never told which instrument produces the higher result.

Similar to the response to the previous comment, we have added specifically which instrument produces higher results:

“As discussed in Section 2, reflectance measured by RSP is larger than SPEX Airborne measurement by a systematic difference of 4% and 3% at 410 and 470 nm respectively.”

Meanwhile in the same paragraph, we showed how much impact on the Rrs could come from the systematic difference on the bands of 410 and 470nm, and why we excluded the wavelength less than 470nm in Rrs comparisons. We added more discussions here:

“The reflectances measured by RSP at 410 and 470 nm are 0.15 and 0.09, respectively. Based on the definition of Rrs, the 4% and 3% systematic difference in the reflectance will transfer into a large Rrs biases around 0.002 and 0.0009 sr⁻¹. Therefore the Rrs from both RSP and SPEX at wavelengths less than 470nm are not compared...”

4. Theoretical retrieval uncertainty and validation against measurements

The authors to their credit address uncertainty from both the theoretical perspective and then also by comparing with ground-based measurements with well-defined uncertainty. The act of validation validates the magnitudes of the retrieved properties.

In addition the act of validation validates the theoretical estimate of the uncertainties.

The authors should explain explicitly in the paper when the theoretical polarimeter uncertainty is validated by the ground-based measurements and when it is not. I never believe the calculations of theoretical uncertainty until validation. On P17 Lines 11-12, “These reduced uncertainties in the aerosol micro-physical properties can help to determine aerosol type and its composition..” The authors here are discussing the theoretical reduced uncertainties. Have these reduced uncertainties been explicitly validated?

Thank you for the comments on validations. To make our discussion more accurate, we revised the corresponding statement by referring to explicitly “retrieval accuracy”, and “retrieval uncertainties”, and added the limitation in validation data and the requirement of future validation campaigns:

“Meanwhile, we have shown polarization information can help to improve retrieval accuracy in the retrieval of aerosol optical depth, fine mode refractive index and SSA as shown in Fig. 5. Besides the theoretical retrieval accuracy analysis, validations with direct measurements are important to account for unknown uncertainties. The AOD results from polarimetric retrievals can be validated with ground-based measurement such as AERONET and lidar measurements such as HSRL, however, it is challenging to validate complex aerosol refractive index, SSA, and size distribution for the entire atmospheric column due to the lack of direct measurements. Such validation requires well-planned airborne field campaigns, concepts for which are under development (PACE validation plan 2020)”

The concern I have is that the authors believe their theoretical calculations of uncertainty too much. P16 Lines 3-5. “Note that AERONET aerosol product uncertainties are approximately 0.01 for AOD, 0.05 for refractive index, and 0.05-0.07 for SSA as mentioned in Section 2, which are comparable with the results for $7\rho_t$ but larger than the ones from $7\rho_t + 5\rho_t$. “ The implication is that RSP is more accurate than AERONET. There might be argument that RSP SSA retrievals are more accurate

than AERONET inversion, but there is no way the RSP retrievals of AOD are going to be better than the AERONET direct sun measurements.

The point is that theoretical uncertainty calculations can only calculate the uncertainty that is known and when a retrieval is made in the real world, then the uncertainty that cannot be quantified theoretically, enters the picture and the actual accuracy of the retrieval is less good than the theoretical calculation.

This is a very good point. We revised our manuscript as in the response to previous comments with acknowledgement of the limitation of the theoretical uncertainty and the necessary for more direct validation, which is repeated as follows:

“Meanwhile, we have shown polarization information can help to improve retrieval accuracy in the retrieval of aerosol optical depth, fine mode refractive index and SSA as shown in Fig. 5. Besides the theoretical retrieval accuracy analysis, validations with direct measurements are important to account for unknown uncertainties. The AOD results from polarimetric retrievals can be validated with ground-based measurement such as AERONET and lidar measurements such as HSRL, however, it is challenging to validate complex aerosol refractive index, SSA, and size distribution for the entire atmospheric column due to the lack of direct measurements. Such validation requires well-planned airborne field campaigns, concepts for which are under development (PACE validation plan 2020)”

5. The results question the ability of PACE to produce Rrs at short wavelengths P20 Line 2. “The resulting hyperspectral water leaving reflectances agree well with the AERONET OC and MODIS OC products.” Well, not towards the blue, near 470 nm. Hasn’t this always been the problem? Ocean biology products need water leaving radiance at the short wavelengths, and they are going to want the UV also. Here the authors show that towards the blue, the hyperspectral retrieved water leaving radiance deviates from AERONET and MODIS products by a lot. At 470 nm for the 10/23 case, the SPEX airborne retrieved remote sensing reflectance is half of what AERONET-OC measured. This does not bode well for the ability to use the blue and UV from the PACE hyperspectral Ocean Color Instrument in any reliable, consistent fashion. The authors examine two cases. In one out of the two cases the atmospheric correction fails at shorter wavelengths for the hyperspectral retrieval. This needs to be stated explicitly when describing Figure 6, but also explicitly in the Conclusions.

Thank you for the comments. In the response to comment 1 (repeat below), we revised statement on the comparison of RSP, SPEX and AERONET Rrs in the conclusion:

“...
The retrieval uncertainties on RSP Rrs is within 0.0004 sr^{-1} (same to SPEX Rrs), while the comparison of the two cases with the AERONET Rrs shows a difference less than 0.0003 sr^{-1} for RSP Rrs, and a maximum difference of 0.0004 sr^{-1} (Case 10/25) and 0.001 sr^{-1} (Case 10/23) for SPEX Rrs. The difference of SPEX Rrs for Case 10/23 is larger than

the retrieval uncertainties, which is likely due to the radiometric uncertainties from the sensors.

“

Meanwhile, MAP radiometric measurements are expected to have higher agreement with PACE OCI through cross-calibration, as discussed in section 5(second paragraph):

“...On-orbit MAP cross-calibration with OCI will be possible – for example, measurements at the $\pm 20^\circ$ viewing angle of SPEXone are expected to be cross-calibrated with OCI, transferring the high radiometric accuracy from OCI to SPEXone (Werdell et al 2019)”

The following discussion are added in the conclusion to clarify the implication to PACE OCI:

“Although the hyperspectral atmospheric correction for wavelength less than 470nm cannot be demonstrated by the SPEX airborne data, the PACE OCI will provide high quality hyperspectral measurement from 340 to 890nm and a few SWIR bands, and the demonstration of the atmospheric correction including UV spectral range will require future studies. “

More detailed comparison of the Rrs spectrum has been provided in the discussion of Figure 6

“... The RSP Rrs at 470 and 550nm are 0.0026 and 0.0020 respectively for Case 10/23, and 0.0025 and 0.0021 respectively for Case 10/25 as shown in Table 3. For AERONET Rrs, the values at 442, 490 and 550nm are 0.0027, 0.0028, 0.0017 sr^{-1} for Case 10/23, and 0.0028, 0.0029, 0.0017 sr^{-1} for Case 10/25. Using the interpolated value of AERONET Rrs at RSP bands, the difference between RSP and AERONET Rrs are within 0.0003 sr^{-1} .”

More discussions on the comparison of SPEX and AERONET Rrs are in the revised file and diff file.

6. Smaller items, but some are still substantial

Abstract Line 4. “aerosols properties” should be “aerosol properties”

Done

P6 Line 19. “water leaving reflectance”. Is the same as Remote Sensing reflectance mentioned on Line 16? The terms seemed to be used interchangeably, and I’m not sure that is correct.

Thanks for pointing this out. We revised the “water leaving reflectance” as “water leaving signals”. The definition of the water leaving reflectance is provided in Eq(2), and its connection with Rrs is in Eq(1).

Figure 6 caption. What do the error bars signify?

We revised the caption as follows:

“The error bars for the RSP retrieved results with cost functions of 7pt and 7pt+ 5Pt indicate one sigma retrieval uncertainties. SPEX Airborne atmospheric correction use the same RSP retrieved aerosol models and therefore shares the same retrieval uncertainties (not indicated in plot). The error bar for the AERONET OC Rrs indicates its daily variation.”

P8 Line 8. “uncertainties” is misspelled.

Corrected.

P9 Line 9. Does the rho_Sensor need a ‘w’ subscript?

Yes, thank you for spotting this. Corrected.

P9 Lines 13-15. That statement, “_Sensor w represents the water leaving signals originating from scattering in the ocean, and can be derived from the atmospheric correction process by subtracting the reflectance contribution of atmosphere and ocean surface from the measurement at the aircraft (Gao et al., 2019).” This statement warrants an explicit equation so that the reader does not need to look up the reference. Maybe repeat from the Mobley reference also.

Thanks for the suggestion. We added a formula for it:

“The water leaving reflectance ρ_w^{Sensor} represents the signals originating from scattering in the ocean and reached the sensor, and can be derived from the atmospheric correction process as $\rho_w^{Sensor} = \rho_t - \rho_{t,atms+sfc}^{Sensor}$ where $\rho_{t,atms+sfc}^{Sensor}$ is the reflectance contribution of atmosphere and ocean surface at the aircraft (Mobley et al 2016, Gao et al 2019)”

P9 Lines 26-27. “The total amounts of water vapor and oxygen are computed from minimizing the difference between measurement and simulated SPEX Airborne measurement over all the bands. “ This statement could be expanded upon to provide greater clarity.

Thank you for the suggestion. We revised the statement as follows:

“We then simulated the reflectance spectra under SPEX geometries with the retrieved aerosol properties and various amounts of oxygen and water vapor. The simulated spectra are compared with SPEX Airborne measurement, and the best amounts of water vapor and oxygen are chosen to minimize the difference between the measurements and simulations. During this process the aerosol properties and ozone density are kept unchanged. “

P9 Line 32. “Each parameter was varied within a boundary as specified in Gao et al. (2018).” Could we have the details repeated here? The authors draw heavily upon references to their previous publications, which is fine, but these details need to be repeated here to make this paper complete in its own right.

We revised the sentence to provide the range of the key parameters:

“Each parameter was varied within a boundary as specified in Gao et al. (2018 and 2019), where the wind speed is less than 10 m/s, the Chlorophyll a concentration is less than 30 mg/m³, the aerosol refractive index varies effectively between 1.3 to 1.6 in its real part and between 0 to 0.03 in its imaginary part, and random mixing fractions of the five aerosol volume densities constrained by a maximum total AOD of 0.3.”

P10 Lines 5-6. “viewing angles on the glint side, and the negative viewing zenith angles refer to the sun side.” Isn’t the glint and the sun on the same side? Glint is forward scattering. This confusion continues throughout. The paper needs this clarified.

We revised the Figure 1 caption by pointing out that the asterisk symbol indicate the antisolar point, we then revised the above statement as :

“...the negative viewing zenith angles refer to the antisolar point in Figure 1b. ... the reflectance and DoLP are simulated and compared with the measurements as shown in Fig. 2 and Fig. 3, where the viewing zenith angles are the same as defined in Figure 1(b) with the positive sign referring to the glint side ($\phi < 90^\circ$ or $\phi > 270^\circ$), and the negative sign referring to the other hemisphere containing the antisolar point.”

Table 3 caption. “parenthesis” should be parentheses. Plural.

Corrected

P15 Lines 10-12. “The coarse mode SSAs are of 0.7 – 0.8 for both days and both cost function options. Moreover, including polarization in the retrievals, the uncertainties for refractive index, SSA and AOD become 0.02 – 0.03 for refractive index, 0.02 – 0.04 for SSA, and 0.004 for AOD, which are reduced nearly by one half.” Because these two sentence run one after the other, the second sentence appears to refer to the coarse mode, but the numbers seem to represent the conditions of the fine mode.

Thank you for the comments. The sentences are revised as follows:

“For the fine mode, when including polarization in the retrievals, the uncertainties become 0.02 – 0.03 for refractive index, 0.02 – 0.04 for SSA, and 0.004 for AOD, with most values reduced by more than one half. The uncertainties for most coarse mode properties remain with similar magnitudes.”

P16 Line 13. “in situ measurements”. The MODIS retrievals are certainly not in situ measurements, and it is debatable whether we should be calling the AERONET

SeaPRISM measurements “in situ”. Possibly for SeaPRISM.

Thanks for the suggestion. We revised the sentence as:

“The results are compared with the MODIS OC products and the SeaPRISM measurements from AERONET OC in Fig.6”

P17 Lines 5-6. “The difference of the MODIS and SPEX Rrs at wavelengths smaller than 500 nm may be related to the measurement uncertainties where the effects are larger for the same percentage uncertainties due to the larger total measurement values.” I did not understand this sentence at all.

We revised the sentences as follows:

“The larger difference of RSP, SPEX and MODIS Rrs at wavelengths smaller than 500 nm may be related to the measurement uncertainties where the reflectance are larger at shorter wavelengths.”

P18 Line 7. VIS is never previously defined. Just write out “visible”

Done.

P18 Line 10-11. “Meanwhile, we have shown polarization information can help to improve accuracy in the retrieval of aerosol optical depth, fine mode refractive index and SSA as shown in Fig. 5.” I actually see the opposite in Figure 5 for SSA, at least the retrieval without polarization gets closer to AERONET retrievals, but really how can we believe any of it when AOD is less than 0.04?

Here we intended to discuss the retrieval uncertainties, and we revised the sentences as follows:

“Meanwhile, we have shown polarization information can help to reduce retrieval uncertainties in the retrieval of aerosol optical depth, fine mode refractive index and SSA as shown in Table. 3, but the retrieval accuracies are limited by the low AOD.”

We also revised the statement in the conclusion to mention the disagreement with AERONET SSA:

“The absolute values also agree better with the AERONET aerosol product except SSA probably due to the large uncertainty of SSA from both the MAP and AERONET inversions at low AOD”.

P18 Lines 21-23. Do the authors really believe this? I find it very far-fetched that they are trying to assign type to an aerosol with AOD less than 0.04. Really? The Russell study was using a data base where the entries all had significant loading. Whatever they found would have no relationship to the cases of the present study, because the

present study is way outside of the Russell study's dynamic range. This speculation should just be removed from the paper.

Thanks, we removed the discussion on aerosol typing.

Figure 7 is never referenced in the text.

Figure 7 is referred in page 19.

P19 Line 16. "The absolute values also agree better with the AERONET aerosol product." Not true for SSA.

The sentence is revised as follows (as mentioned previously):

"The absolute values also agree better with the AERONET aerosol product except SSA probably due to the large uncertainty of SSA from both the MAP and AERONET inversions at low AOD".

P19-20 Lines 20-2. "In order to apply the retrieved aerosol properties from the MAP measurements to hyperspectral atmospheric correction, the principal components of the aerosol refractive index spectra are interpolated into the bands specified for SPEX airborne. The retrieval parameters from MAP measurements can be used directly with the hyperspectral measurements without interpolation." The two sentences are contradictory. The first states that the refractive index spectra have to be interpolated into hyperspectral. The second states that no interpolations is necessary.

Thank you for the comments. The interpolation is referred to the principal components of the refractive index spectra, each principal component is a spectrum. We removed the second sentence since the principal component coefficients cannot be interpolated.

Response to the report of reviewer #3:

We appreciate the detailed comments and suggestions from the reviewer, which are very helpful in improving the clarity of this work. Please find our responses with corresponding revisions below.

Interactive comment on “Inversion of multi-angular polarimetric measurements from the ACEPOL campaign: an application of improving aerosol property and hyperspectral ocean color retrievals” by Meng Gao et al.

Anonymous Referee #3 Received and published: 6 April 2020

The study aims at demonstrating the benefit of using synergistically hyperspectral and multi-angular polarimetric (MAP) observations to improve ocean color remote sensing, especially in the coastal zone, where aerosols are complex, relatively abundant, and highly variable. The approach is to use aerosol properties (size distribution parameters, index of refraction, optical thickness) retrieved from MAP data in a forward radiative transfer model to estimate the aerosol signal, therefore perform atmospheric correction of the hyperspectral measurements. To achieve this objective RSP and SPEX aircraft measurements acquired off the West Coast of California were used, and the retrievals of aerosol properties and, therefore, remote sensing reflectance were compared with AERONET-OC measurements. Uncertainties in aerosol retrievals are reduced substantially (factor of 2) when using polarization and reflectance instead of just reflectance data, and the retrieved quantities show some agreement with in-situ measurements. The authors conclude that the findings constitute a proof-of-concept for the PACE mission, i.e., MAP data would be used in a similar way to correct atmospheric influence on the OCI hyperspectral imagery.

The approach is technically sound, the inversion techniques appropriate and robust, and the data processing/analysis performed carefully, but several issues prevent publication of the manuscript. First, aerosol abundance during the flights analyzed is very small, i.e., about 0.02 at 865 nm. With such minimum loadings, the signal to correct is so small that even large errors in the aerosol model would still yield sufficient accuracy on the remote sensing reflectance. It is not surprising, therefore, that even though differences are relatively large between estimates of size distribution, real part of index of refraction, and single scattering albedo using 7rhos and 7rhos + 5Pols (e.g., Figure 5), the retrieved RSP remote sensing reflectance is similar. I suspect that simply using the aerosol information from the MERRA-2 data would have provided similar performance. In other words, the demonstration is not credible when using cases with almost no aerosols.

Thanks for the summary and the positive comments in our approach and analysis. Also thanks for the discussions on the small AOD in our study. Here we provide more clarifications here:

- 1) We agreed that the aerosol loadings in these two cases are small which is about 0.03-0.04 at 550nm, and 0.02-0.03 at 865 as the reviewer corrected pointed out. However, due to the small value of the remote sensing reflectance, accurate retrieval of the aerosol properties is still important to determine the remote sensing reflectance. As verified from radiative

transfer simulations with aerosols only, aerosol reflectance contributes to the same order of magnitude as the remote sensing reflectance at 400-550nm range. The following discussions are provided and revised in the Section 2 (second last paragraph):

“...Although the aerosol loading is small, its contribution is of the same order of magnitude as the water leaving signal between 400-550 nm range, and hence remains important for atmospheric correction. Therefore, both the retrieval of aerosol micro-physical properties and the water leaving signals require high accuracy of the measurements from RSP and SPEX Airborne.”

- 2) We agree that the similar remote sensing reflectance obtained using the aerosol properties obtained from the two different cost function may relate to the small optical depth, and several other factors. Please note that the available cases with co-located multi-angle polarimetric measurement and hyperspectral measurements are really rare. We revised our manuscript to state the importance for future studies and validation campaigns with various aerosol loading. Some discussions and revisions are provided in Section 5 (third paragraph):

“Meanwhile, we have shown polarization information can help to improve retrieval accuracy in the retrieval of aerosol optical depth, fine mode refractive index and SSA as shown in Fig. 5. Besides the theoretical retrieval accuracy analysis, validations with direct measurements are important to account for unknown uncertainties. The AOD results from polarimetric retrievals can be validated with ground-based measurement such as AERONET and lidar measurements such as HSRL, however, it is challenging to validate complex aerosol refractive index, SSA, and size distribution for the entire atmospheric column due to the lack of direct measurements. Such validation requires well-planned airborne field campaigns, concepts for which are under development (PACE validation plan 2020)”

- 3) Thank you for suggesting the use of MERRA2 aerosol model for atmospheric correction. We conducted the following evaluations:
 - a. We located the corresponding MERRA2 one hour aerosol product as archived in <https://oceandata.sci.gsfc.nasa.gov/> for the two cases in our study at 2017/10/23 21:33 and 2017/10/25 21:07 (file names are N201729621_AER_MERRA2_1h.nc and N201729821_AER_MERRA2_1h.nc).
 - b. We then located the MERRA2 pixels near the AERONET SeaPRISM site location and found that the corresponding MERRA2 AOD are 0.054, and 0.080 at 550nm for cases 10/23 and 10/25. Note that AERONET AOD at 550nm are 0.034, while HSRL AOD at 532nm are 0.036 similar to both days. Our retrieved AODs at 550nm are 0.033 for Case 10/23 and 0.031 for Case 10/25. The MERRA2 AOD overestimate AERONET AOD by 0.02 and 0.046 respectively.
 - c. We estimated the amount of aerosol contribution to the remote sensing reflectance (ΔR_{rs}) by using the single scattering approximation, namely, $\Delta R_{rs} \sim AOD \times B/\pi$, where B is the aerosol backscattering fraction at 550nm (around 0.2 for our cases). We have $\Delta R_{rs} \sim 0.001$ and 0.003 for Case 10/23 and 10/25 respectively, larger than the difference (< 0.0005) between our retrievals and the AERONET Rrs at 550nm, especially for case 10/25.

d. Therefore, we concluded that MERRA2 aerosol model is not ideal for the atmospheric correction in our studied cases. However, the suggestion to investigate MERRA2 aerosol model is interesting. We can study whether MERRA2 aerosol model can be used as a way to better select initial values in the retrieval algorithm in our future study.

Second, HARP2 on the PACE mission will not measure in the shortwave infrared, so the demonstration should have been made using 5rhos and 5rhos + 5Ps to better mimic/represent the PACE capabilities.

Thank you for the suggestion on removing SWIR bands in aerosol retrievals. In this study we aim to provide best retrievals using the full capability of the RSP sensors, although DoLP measurements in SWIR bands are not used due to issues discussed in the manuscript. We did not intend to make RSP measurements to look the same as HARP or SPEX. Even after we removed the RSP SWIR bands, RSP are still different than HARP and SPEX with many more viewing angles and different measurement uncertainties. However, the algorithm and procedures using the current RSP measurements can be applied to other polarimetric measurements as a proof of concept demonstration to assist hyperspectral atmospheric correction. Furthermore, there are SWIR measurement in PACE OCI, which may have higher SNR, and it is potentially can be used to assist the MAP retrievals. We revised our manuscript as follows:

“The percentage uncertainties of the polarizations in the two SWIR bands further increases when the DoLP value decreases. We have tested the effects of the DoLP at the two SWIR bands on the aerosol retrieval and found that including them does not improve the retrieval accuracies, so the SWIR DoLPs are not used in our retrievals. Moreover, the PACE MAPs do not include polarimetric SWIR measurements but PACE OCI includes several SWIR bands measured at a single viewing angle and may have higher accuracy, a synergy of PACE OCI SWIR with MAP measurements may further improve aerosol retrievals.”

Furthermore, no comparison was made with remote sensing reflectance retrievals performed by the standard algorithm applied to aircraft RSP and SPEX data (possible even though for SPEX the spectral range is limited in the near infrared), in order to evaluate potential improvements by the proposed method.

This is another good suggestion to apply standard atmospheric correction algorithm on RSP and SPEX data. However, this requires generating appropriate aerosol lookup table for the exact RSP and SPEX bands which are not currently available in the processing software. This suggestion deserves a separate study which is out of scope of this work.

Finally, examining Figure 6, one cannot convincingly conclude that SPEX-derived hyperspectral reflectance in the blue agree with the in-situ measurements, i.e., in Section 4 the statement “The resulting hyperspectral water leaving reflectances agree well with the ARONET OC and MODIS OC products” is incorrect.

Thank you for the comments. We made the following revisions to provide more details:

“...

The retrieval uncertainties on RSP Rrs is within 0.0004 sr^{-1} (same to SPEX Rrs), while the comparison of the two cases with the AERONET Rrs shows a difference less than 0.0003 sr^{-1} for RSP Rrs, and a maximum difference of 0.0004 sr^{-1} (Case 10/25) and 0.001 sr^{-1} (Case 10/23) for SPEX Rrs. The difference of SPEX Rrs for Case 10/23 is larger than the retrieval uncertainties which is likely due to the radiometric uncertainties from the sensors.

“

We have also added more discussions on the difference between RSP Rrs, SPEX Rrs and AERONET. On the comparison between RSP and AERONET Rrs:

“... The RSP Rrs at 470 and 550nm are 0.0026 and 0.0020 respectively for Case 10/23, and 0.0025 and 0.0021 respectively for Case 10/25 as shown in Table 3. For AERONET Rrs, the values at 442, 490 and 550nm are 0.0027, 0.0028, 0.0017 sr^{-1} for Case 10/23, and 0.0028, 0.0029, 0.0017 sr^{-1} for Case 10/25. Using the interpolated value of AERONET Rrs at RSP bands, the difference between RSP and AERONET Rrs are within 0.0003 sr^{-1} .

...”

More discussion on comparison of SPEX Rrs and AERONET Rrs can be found in the revised file and the diff file.

The above criticisms notwithstanding, the study is interesting. The procedures for estimating the atmospheric interference are well defined. I would recommend showing retrievals over the entire 2 flights (along and perpendicular to the coast) to capture varied aerosol and water reflectance situations, even though in situ measurements may not be available, compare the remote sensing reflectance retrievals with those of the standard algorithm, and evaluate against the aircraft lidar measurements and satellite products, but this would require a new submission.

Thank you for the interest in the study and the suggestions to include the whole flight retrieval.

We have conducted studies on a flight track over water of day 10/23, and compared the retrieved RSP AOD (with polarization measurement) with the HSRL AOD as shown in the Figure 1 below. Over the flight track, the AOD variations are very small mostly around 0.02-0.04 (HSRL 532nm). For the day of 10/25, there are a limited number of pixels over water for analysis (plot not shown), and the AOD are around 0.03~0.05(HSRL 532nm). Therefore we are not discussing these results in the manuscript to capture aerosol variations, instead we only focus on the representative cases. For the study using standard atmospheric correction algorithm, as we have discussed previously, it requires new development of lookup table which is outside current study scope.

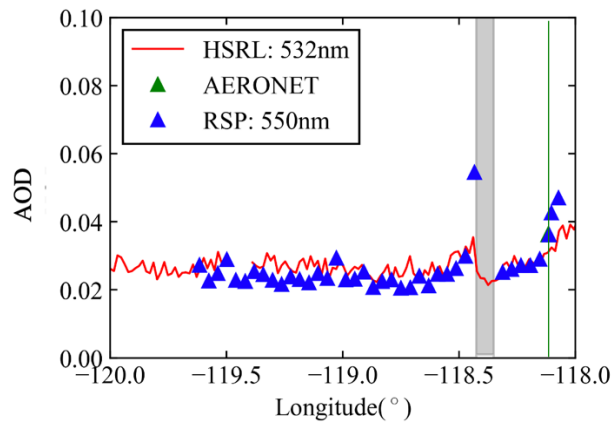


Figure 1. Retrieved RSP AOD and the HSRL AOD for Day 10/23. The green line indicates the location of the AERONET site where AERONET AOD coincides with the retrieved RSP AOD; grey area indicates the location of the island with data screened.

Response to the report of reviewer 2:

Thank the reviewer for the valuable suggestions and comments, which improve the clarity of this work significantly. On the technical correction/improvements, the figures and table have been updated and captions have been revised. On the scientific correction/improvements, the comments have been addressed below and the manuscript is revised accordingly.

This manuscript provides uses actual, airborne data sets obtained from the ACEPOL campaign to describe a proof-of-concept method for ocean color retrievals from the polarimeters and hyperspectral imagers onboard the 2022 NASA/PACE mission. The objectives, data sets, retrieval method, and validation efforts are explained clearly, and the subject of this manuscript falls well within the scope of AMT. Therefore, this manuscript is suitable for access review. The comments below provide suggestions and questions to improve the technical and scientific qualities of this manuscript

Suggestions for technical corrections/improvements:

1. **Fig 1b:** provide symbols for the polar angles that identify the numbers in this polar plot. Also, use a less-confusing definition for the asterisks (e.g., “back-scattering direction” or “sunglint” instead of “solar direction”)
Provided. The relative azimuth and zenith angles are indicated by ϕ and θ in the plot. Asterisk symbol indicates the antisolar point as revised in the figure caption.
2. **Fig. 4a:** mark the “ $(\text{Chi}_{\text{min}})^2$ ” values described in the text
The minimum cost function values are indicated by arrows in both Fig 4a and 4b (for consistency).
In order to align $(\text{Chi}_{\text{min}})^2$ with the left edge of the first bin in the histogram, the histogram and cumulative probabilities are recomputed using bins from $(\text{Chi}_{\text{min}})^2$ instead of zero as previously used.
3. **Table 3:** add “AOD(fine)” and “AOD(coarse)” for the optical thickness of fine-mode and coarse-mode aerosol, respectively
Both fine and coarse mode AOD are added.

Suggestions for scientific corrections/improvements:

1. **Page 2, Lines 15-16:**
“... improve the retrieval performance of aerosol microphysical properties (Mischenko and Travis, 1997; ...”
►
“... improve the retrieval performance of aerosol microphysical properties (Mischenko and Travis, 1997; Chowdhary et al., 2001; ...”
Added. Thank you for suggesting the reference.

2 Page 2, Line 24:

“... and National Aeronautics and Space Administration (NASA)’s Multi-Angle ...”



... the National Aeronautics and Space Administration (NASA) Multi-Angle ...
Updated.

3 Page 3, Lines 11-14:

“... To date, the procedures for using MAP data to aid the hyperspectral atmospheric correction of collocated ocean measurements ... has not yet been demonstrated. ...”

Comment:

This is not true: see <https://ui.adsabs.harvard.edu/abs/2018AGUFMOS11D1435C/abstract>. The lead authors of the current submitted manuscript may recall that they visited that AGU presentation and engaged in discussions. The citation is: Chowdhary, J., Stamnes, S., Zhang, M., Scarino, A.J., Wasilewski, A.P., Cairns, B., “Combining multispectral VIS-SWIR polarimetry and UV-NIR hyperspectral imagery to retrieve aerosol and ocean color properties from remote sensing: case studies for airborne RSP and GCAS observations”, American Geophysical Union, Fall Meeting 2018, abstract #OS11D-1435

Thank you for the comments and reminding us the interesting work. We revised the manuscript as follows:

“... To date, there are only a few studies on performing atmospheric correction for hyperspectral radiometer using aerosol properties retrieved from the co-located MAP measurements. This is primarily due to the limited availability of co-located MAP and hyperspectral radiometer measurements over ocean. One such dataset is available from the North Atlantic Aerosols and Marine Ecosystems Study (NAAMES) field campaign in 2015, where both the GEO-CAPE Airborne Simulator (GCAS) (a hyperspectral radiometer) and RSP were deployed. These datasets have been used to study the hyperspectral ocean color retrievals (Chowdhary et al. 2018).”

4 Page 4, Lines 8-9:

“... advantageous in scenarios where the aerosol properties in the VIS or ultraviolet (UV) bands cannot be accurately extrapolated from measurements in the NIR-SWIR spectral range.”



“... advantageous in scenarios where the aerosol properties in the VIS or ultraviolet (UV) bands cannot be accurately extrapolated from measurements in the NIR-SWIR spectral range (Chowdhary et al., 2019).”

Added. Thanks.

5 Page 6, Line 20:

“... depends on the polarization state and the water conditions (Zhai et al., 2017).”



“... depends on the wavelength and the water conditions (Chowdhary et al., 2012; Zhai et al., 2017).”

Citation:

Chowdhary, J., B. Cairns, F. Waquet, K. Knobelispiesse, M. Ottaviani, J. Redemann, L. Travis, and M. Mishchenko, 2012: Sensitivity of multiangle, multispectral polarimetric remote sensing over open oceans to water-leaving radiance: Analyses of RSP data acquired during the MILAGRO campaign. *Remote Sens. Environ.*, **118**, 284-308, doi:10.1016/j.rse.2011.11.003.

Added. Thanks.

6 Page 7, Lines 8-9:

“... where the waters are mostly clear so that the bio-optical model parameterized by Chlorophyll-a concentration is used. ...”

Comment:

Clear waters do not always imply that their IOPs co-vary with the Chlorophyll-a concentration. For example, one of the clearest ocean waters are found off the West Coast of South America. These waters exhibit also a large deficiency in CDOM compared to other open ocean waters with the same Chlorophyll concentration (Morel, Claustre, Antoine, and Gentili, 2007; Morel, Gentili, Claustre, Babin, Bricaud, Ras, and Tièche, 2007). Given that the SPEXone-derived Rrs values so low in the blue spectrum when compared to MODIS and AERONET for Case 10/23 (see Fig. 6), might it be that this 1-parameter bio-optical model was not appropriate for this case study? In other words, did the authors also consider Rrs retrievals using their multi-parameter bio-optical model?

Thanks for the discussion. The multi-parameter bio-optical model proposed in our previous work (Gao et al, OE, 2018) was also investigated, but due to the small water leaving signals, there are large uncertainties associated with this complex model. A similar example has been demonstrated in Gao et al, AMT, 2019. The Rrs from RSP with one-parameter bio-optical model discussed in this study agree well with the in-situ AERONET OC product. Note that the Rrs from SPEX use the same aerosol properties retrieved from RSP to conduct atmospheric correction.

7 Page 7, Line 13:

“... For a general study, Fu et al discussed ...”



“... For a general study, Fu and Hasekamp discussed ...”

Updated. Thanks.

8 Page 10, Lines 20-21:

“... which indicates the measurements cannot be modelled by the forward model ...”

Comment:

One possibility may be a change of residual sunglint in nadir-viewing direction that is caused by wind-directionality of the ocean surface roughness. This is consistent with the reflectance results at 2250 in Figure 3(a) (which are predominantly sensitive to coarse-mode aerosols and sunglint contamination), and with the comments made in page 13, lines 10-11, on the sensitivity of sunglint to wind speed.

We agree with the reviewer. Page 9, line 1-3 discussed that a scalar wind speed which represents an isotropic Cox-Munk model may be not sufficient to model the sunglint in this study. This is the reason why the sunglint data is not used in the current retrievals.

9 Page 13, Line 5:

“... SSA spectra for both fine and coarse modes ...”

Comment:

Table 3 reports also the total SSA. How is this SSA value computed from those reported for the fine and coarse mode aerosols?

We added a sentence to define the total SSA following Bohren and Huffman(1998, page 445):

“The overall SSA for the two mode mixture is computed as the ratio of the number density weighted averages for the scattering and extinction cross sections (Bohren and Huffman, 1998).”

10 Page 15, Line 8:

“... which agree better with the AERONET results of 1.6. ...”

Comment:

Aren’t the AERONET retrievals assuming the same refractive index for the fine- and coarse-mode aerosols? Wouldn’t this make the AERONET refractive index retrieval more sensitive to the dominant aerosol mode? To better assess the comparison of refractive index (and SSA!) retrievals with the AERONET products, Table 3 could therefore also report retrieval results AOD(fine) and AOD(coarse). This will allow one to compute a weighted refractive index and compare this with AERONET retrievals akin to Hasekamp et al. (2011).

Thanks for the suggestion. In order to be consistent with the reference of Hasekamp et al. (2011) and our previous study in Gao et al (2018), we computed the volume averaged refractive index and made the following revision in the manuscript:

“To compare with the AERONET refractive index which assumes both modes are the same, we define the volume-averaged refractive index as $mv=fv * mr(fine)+(1-fv) * mr(Coarse)$ where fv is the fine mode volume fraction (Hasekamp et al 2011, Gao et al 2018). For Cases 10/23 and 10/25 with $7rho_t$, mv is 1.49 and 1.48 respectively. While with $7rho_t+5P_t$, mv becomes 1.58 and 1.56 for these two days, which agree better with the AERONET refractive index of 1.6.”

11 Page 16, Lines 19-20:

“... The RSP and SPEX Rrs at wavelengths shorter than 470 are not compared due to the large absolute systematic difference in the 410 and 470 nm bands as discussed in Section 2. ...”

Comment:

Why choosing to exclude the results for 410 nm? Since both the 410 and 470 nm bands show systematic differences, it makes more sense to either exclude, or include, results for *both* these bands.

Thank you for the question. We clarified this in the following revisions:

“The RSP 410nm band is excluded from comparison due to the observation of 4% decrease in its radiometric throughput, while other RSP bands maintain stable within ~ 1% in the radiometric calibration and ~ 0.1% in the polarimetric calibration (Knobelspiesse et al, The Aerosol Characterization from Polarimeter and Lidar (ACEPOL) airborne field campaign, to be submitted). The SPEX Rrs at wavelengths shorter than 470 nm are not compared because of the observed absolute systematic difference comparing with the RSP 410 and 470 nm bands as discussed in Section 2.”

12 Page 16, Line 22:

“... Case 10/25 shows good agreement between SPEX Airborne, RSP, ...”

Comment:

Specifically, this is also true for the 470 band. So why is this not true for the 470 band in Case 10/23, even after assigning an uncertainty bar for SPEX retrievals that is the same as the uncertainty bar for RSP retrievals in coinciding bands? Both these cases are only 2 days apart, which suggests that the absolute systematic difference between SPEX and RSP radiance measurements in the 470 band is the same for these days and can therefore not be the only cause for the disagreement in their Rrs retrievals.

Thank you for the comments. As the reviewer correctly pointed out that SPEX and RSP Rrs at 470nm agrees better in 10/25 than 10/23. Since the atmospheric correction for both RSP and SPEX use the same aerosol models retrieved from RSP, the difference in Rrs is more likely originated from the difference in their radiometric measurements. Note that the systematic and random difference between RSP and SPEX at 470nm band is 3% and 2% as shown in Table 2, Smit et al, 2019. We added the following discussion in the manuscript:

“Based on the definition of R_rs, the 4% and 3% systematic difference in the reflectance will transfer into Rrs biases around 0.002 and 0.0009 sr⁻¹. The random difference between RSP and SPEX measurements at 470nm band is 2% as discussed by (Smit et al 2019) which can transfer to 0.0006 sr⁻¹ in Rrs. The differences of the R_rs} from RSP and SPEX at 470nm (0.0012 for Case 10/23 and 0.0003 for Case 10/25 with 7\rho_t+5P_t) may be due to the combined effects of the random and systematic differences in their measurements.”

12 Page 17, Lines 4-5:

“... and the MODIS Rrs is in between ...”

Comment:

Note that the MODIS and AERONET retrievals do not even agree with each other within their reported error bars. This suggests that the reported error bars for the MODIS and/or AERONET products are too small, which complicates a comparison with RSP/SPEX products. To assess one possible cause for MODIS-AERONET disagreements that is relevant to analyses of SPEX/RSP products, it might be useful to compare aerosol models used for atmospheric correction in MODIS-AERONET-RSP retrievals, and to discuss the impact of their differences on the Rrs retrievals shown in Fig. 6. Including in Fig. 6 the RSP and SPEX retrievals of Rrs for 410 nm would be useful for such a discussion even if RSP and SPEX radiances to not agree for this band (after all, one of them could still be correct).

Thank you for the comments. The difference between SPEX and RSP Rrs have been discussed in the last comment. The reason why RSP 410nm is not used has been discussed in response to comment 11. The differences in their Rrs may due to the uncertainties in the measurement and also possible different aerosol models used for atmospheric correction. We revised the manuscript as follows:

“The difference of RSP, SPEX and MODIS Rrs at wavelengths smaller than 500 nm may be related to the measurement uncertainties where the effects are larger for the same percentage uncertainties due to the larger total measurement values. Another possible reason for the discrepancy between the MODIS Rrs and others is the different aerosol models used for atmospheric correction. For MODIS, it is determined from the two NIR bands of 748 and 869 nm while others are based on polarimeter retrievals.”

Note that the error bar for AERONET and MODIS are computed differently as discussed in section 2, which are generally larger than the reported uncertainties by including temporal and spatial variations. We revised section 2 to make it clearer as follows:

"In order to evaluate the spatial variations when comparing with the retrieved water leaving reflectance, we averaged the MODIS (on board Aqua) water leaving reflectance within a 2km region around the USC_SEAPRISM site and compute its standard deviation as its maximum uncertainty. If smaller than 5%, the uncertainty is adopted as 5% which is the accuracy goal for blue band and clear water (Hu et al 2013). The AERONET measurements are available in almost every hour and there are a total of 8 measurements each day. The AERONET product provides good temporal coverage of the aerosol and ocean reflectance. We averaged the one-day AERONET products and compared its mean with the retrieval results, where the standard deviation (6% to 10% for both Cases) is used to represent the maximum uncertainties. Note that the reported uncertainty for AERONET OC Rrs is approximately 5% between 410- 550nm (Zibordi et al 2009)."

13 Page 17, Line 14:

"... for highly spectrally resolved measurements of the ocean. ..."



"... for hyper-spectrally resolved retrievals of the ocean color. ..."

Thanks for the suggestion. We revised the sentence as:

"...perform an atmospheric correction **on** highly spectrally resolved measurements of the ocean."

14 Page 18, Lines 25-26:

"... The large uncertainties in coarse mode aerosol properties may be due to ... the neglect of the SWIR DoLP in retrievals. ..."

Comment:

This contradicts the statement given **Page 8, Lines 19-20**: "We have tested the effects of the DoLP at the two SWIR bands on the aerosol retrieval and found that including them does not improve the retrieval accuracies".

Thank you for this comment. As shown in Table 2, the total uncertainties in SWIR DOLP measurement are large with values around 6-15% (partly come from the average of five pixels together used in this study). Data with better SWIR DOLP accuracy should help coarse mode retrievals.

We modified the manuscript as follows to be more specific:

"The large uncertainties in coarse model aerosol properties may be due to the small contribution of the coarse mode signal in the total reflectance and the large total uncertainties in the SWIR DoLP (not used in retrievals)."

15 Page 18, Lines 28-34; Page 19, Lines 5-6:

"... This approach provides a statistical evaluation of the uncertainties relating to the cost function sensitivity and impact of initial values. ... The study by Knobelspiesse et al. (2012) estimated retrieval uncertainties using the error propagation method for the Aerosol

Polarimetry Sensor (APS) ... The uncertainties of the retrieval parameters evaluated using random initial values may not represent the full uncertainties in the retrieval. However, the two uncertainty results [...] are comparable, which may relate to the intrinsic sensitivity of the cost functions when converged ...”

Comment:

The authors are upfront and clear about how they compute error bars for the RSP products in this study. A thorough discussion on the merits of this method may fall beyond the scope of this manuscript. However, it is evident that such time-consuming computations, which require performing many retrievals for a single pixel, will not be practical for rapid inversions of PACE data. Rather, solving the cost function in Eq. (1) by means of Jacobians, and computing the error covariance matrix from these Jacobians, not only provides retrieval products but also their associated uncertainties. Given that this study was performed in context of the PACE mission, it might be appropriate that the authors provide a brief comment on this. Furthermore, Knobelpiesse et al (2012), who base their analyses on error covariance matrices, note that their error estimates represent the best possible retrieval uncertainties. Does this then not suggest that the retrieval uncertainties reported in this study are actually underestimated if they compare well with those reported in Knobelpiesse et al (2012)?

Thank you for the comment and suggestions. We have revised the manuscript with more discussions as follows:

“The uncertainty results computed from two different approaches are comparable to each other in magnitudes. The error propagation method directly relates the retrieval uncertainties to the measurement uncertainties by projecting them from measurement to state space using Jacobians calculated from the radiative transfer model. This method accurately represents retrieval uncertainty if: (1) the measurement uncertainty is correct, (2) the forward model is an accurate and complete representation of physical reality, (3) the state space is locally linear about the retrieval, and (4) the retrieval algorithm is able to successfully converge to the smallest cost function value without artifacts. In practice, (2) is nearly always approximate, and (3) and (4) are not always the case, so the methodology used in Knobelpiesse et al. (2012) can be considered the best case retrieval uncertainty. It is, however, a convenient metric for retrieval uncertainty estimation since Jacobians are often calculated as part of the retrieval process and can be reused for this purpose. The retrieval uncertainty method used in this work (expressing the volume in state space containing cost function values calculated with many retrievals performed using randomly generated initial values) is similar in some respects, as it also relies on an accurate measurement uncertainty model (1) and forward model (2). However, it may be more accurate in some cases, since it does not make the assumption of local linearity (3) and can incorporate some potential convergence artifacts (4). Because this technique requires execution of many retrievals, it is computationally inefficient for operational use. It is, however, very relevant for a (data) limited study such as this, as it provides the best possible uncertainty estimate.”

Inversion of multi-angular polarimetric measurements from the ACEPOL campaign: an application of improving aerosol property and hyperspectral ocean color retrievals

Meng Gao¹, Peng-Wang Zhai², Bryan A. Franz³, Kirk Knobelspiesse³, Amir Ibrahim¹, Brian Cairns⁵, Susanne E. Craig³, Guangliang Fu⁶, Otto Hasekamp⁶, Yongxiang Hu⁴, and P. Jeremy Werdell³

¹SSAI, NASA Goddard Space Flight Center, Code 616, Greenbelt, Maryland 20771, USA

²JCET/Physics Department, University of Maryland, Baltimore County, Baltimore, MD 21250, USA

³NASA Goddard Space Flight Center, Code 616, Greenbelt, Maryland 20771, USA

⁴MS 475 NASA Langley Research Center, Hampton, VA 23681-2199, USA

⁵NASA Goddard Institute for Space Studies, New York, NY 10025, USA

⁶Netherlands Institute for Space Research (SRON, NWO-I), Utrecht, The Netherlands

Correspondence: Meng Gao (meng.gao@nasa.gov)

Abstract. NASA's Plankton, Aerosol, Cloud, ocean Ecosystem (PACE) mission, scheduled for launch in the timeframe of late 2022 to early 2023, will carry the Ocean Color Instrument (OCI), a hyperspectral scanning radiometer, and two multi-angle polarimeters (MAPs), the UMBC Hyper-Angular Rainbow Polarimeter (HARP2) and the SRON Spectro-Polarimeter for Planetary EXploration one (SPEXone). One purpose of the PACE MAPs is to better characterize ~~aerosols~~-aerosol properties, which 5 can then be used to improve atmospheric correction for the retrieval of ocean color in coastal waters. Though this is theoretically promising, the use of MAP data in the atmospheric correction of collocated hyperspectral ocean color measurements has not yet been well demonstrated. In this work, we performed aerosol retrievals using the MAP measurements from the Research Scanning Polarimeter (RSP), and demonstrate its application to the atmospheric correction of hyperspectral radiometric measurements from SPEX Airborne. Both measurements were collected on the same aircraft from the Aerosol Characterization 10 from Polarimeter and Lidar (ACEPOL) field campaign in 2017. Two cases over ocean with small aerosol loading (aerosol optical depth ~ 0.04) are identified including collocated RSP and SPEX Airborne measurements and Aerosol Robotic Network (AERONET) ground-based observations. The aerosol retrievals are performed and compared with two options: one uses reflectance measurement only and the other use both reflectance and polarization. It is demonstrated that polarization information 15 helps reduce the uncertainties of aerosol microphysical and optical properties. The retrieved aerosol properties are then used to compute the contribution of atmosphere and ocean surface for atmospheric correction over the discrete bands from RSP measurements and the hyperspectral SPEX Airborne measurements. The water leaving signals determined this way are compared with both AERONET and Moderate Resolution Imaging Spectroradiometer (MODIS) Ocean Color products with good agreement, for performance analysis. The results and lessons-learned from this work will provide a basis to fully exploit the information from the unique combination of sensors on PACE for aerosol characterization and ocean ecosystem research.

1 Introduction

Ocean color remote sensing is a powerful tool for quantifying and monitoring global ocean ecosystems (Dierssen and Randolph, 2013), and provides valuable information for the estimation of phytoplankton biomass (Craig et al., 2012), primary productivity (Carr et al., 2006), and dissolved (Siegel et al., 2014) and particulate carbon pools (Fichot and Benner, 2011). Estimation of the 5 ocean color signal from the total at-sensor space-borne or air-borne measurement is known as atmospheric correction, which removes the radiometric contributions of the atmosphere and ocean surface (Wang, 2010; Mobley et al., 2016). Quantifying the effect of atmospheric aerosols is a primary challenge in the atmospheric correction (Frouin et al., 2019), due to their diversity of size, composition, and morphology, and associated variability in absorption and scattering properties (Remer et al., 2019a). In addition, aerosol deposition into ocean waters contributes to the availability of nutrients that modulate phytoplankton growth 10 and ultimately influence the trophic state of ocean ecosystems (Mahowald et al., 2005; Westberry et al., 2019). Furthermore, the ocean itself and the biological activity it supports may also be a source of aerosol (O'Dowd et al., 2002; McCoy et al., 2015; Croft et al., 2019). Better characterization of aerosol micro-physical and optical properties is expected to improve the retrieved ocean color signal and, therefore, the derived geophysical products that describe ocean ecosystems (PACE, 2018; Werdell et al., 2019).

15 Multi-angle polarimeters (MAPs), radiometers that measure spectral polarization states at multiple view angles, have been demonstrated to improve the retrieval performance of aerosol microphysical properties ([Mishchenko and Travis, 1997](#); [Hasekamp and Landgraf, 2007](#); [Knobelispesee et al., 2012](#)), including for applications over ocean waters (Jamet et al., 2019). A limited number of satellite missions carrying polarimetric payloads have been launched (Dubovik et al., 2019), including the Polarization and Directionality of the Earth's Reflectances (POLDER) 20 instrument that was hosted on Polarization and Anisotropy of Reflectances for Atmospheric Sciences Coupled with Observations from a Lidar (PARASOL; 2004–2013) and on the short-lived ADEOS and ADEOS-II missions (Tanré et al., 2011). Several more satellite missions with MAP instruments are planned to be launched in the time frame of 2022–2023, such as the European Space Agency (ESA)'s Multi-viewing Multi-channel Multi-polarisation Imager (3MI) on Meteorological Operational Satellite - Second Generation (MetOp-SG) (Fougnie et al., 2018), and [the](#) National Aeronautics and Space Administration (NASA) ~~is~~ Multi-Angle Imager for Aerosols (MAIA) (Diner et al., 2018), and the NASA Plankton, Aerosol, Cloud, ocean 25 Ecosystem (PACE) mission (Werdell et al., 2019).

The PACE observatory will include two MAPs, the UMBC Hyper-Angular Rainbow Polarimeter-2 (HARP2) (Martins et al., 2018) and the SRON Spectro-Polarimeter for Planetary EXploration one (SPEXone) (Hasekamp et al., 2019), as well as its primary instrument, a hyperspectral scanning radiometer referred to as the Ocean Color Instrument (OCI). The OCI instrument 30 will provide continuous spectral measurement from the ultraviolet (340 nm) to near infrared (890 nm) with 5 nm resolution, plus a set of discrete shortwave infrared (SWIR) bands centered on 940, 1038, 1250, 1378, 1615, 2130, and 2260 nm. OCI will tilt $\pm 20^\circ$ fore/aft, switching at the sub-solar point, to minimize viewing Sun glint. HARP2 is a wide field-of-view imager that measures polarized radiances at 440, 550, 670, and 865 nm, where the 670 nm band will be at 60 viewing angles and the other bands at 10 viewing angles. SPEXone is a narrow swath imager that performs multi-angle measurements at 5 viewing

angles of 0° , $\pm 20^\circ$ and $\pm 58^\circ$ on ground, in a continuous spectral range spanning 385-770 nm with a resolution of 2-3 nm for intensity, and ~~10-40 nm~~ ~~10-40 nm~~ for polarization (Rietjens et al., 2019).

Through the combination of OCI and the two MAPs, the PACE mission provides a novel opportunity to bridge polarimetric and hyperspectral observations and advance the retrieval of both aerosol and ocean properties (Remer et al., 2019a, b; 5 Chowdhary et al., 2019). Near infrared (NIR) or SWIR bands are often used to derive aerosol properties over ocean waters, and that approach has been implemented for the Hyperspectral Imager for the Coastal Ocean (HICO) (Ibrahim et al., 2018). The multiband atmospheric correction (MBAC) approach which utilizes channels in the NIR to SWIR has been proposed for PACE OCI (Ibrahim et al., 2019). With the PACE instruments, a more accurate retrieval of the aerosol properties can potentially be achieved using the MAP measurements, and the improved aerosol knowledge can then be applied to advance the 10 accuracy of atmospheric correction for OCI observations. This advancement would be especially valuable over coastal waters, where both aerosol and water optical properties are often complex. To date, ~~the procedures for using MAP data to aid the hyperspectral atmospheric correction of collocated ocean color measurements and the performance of such atmospheric correction have not been demonstrated~~ ~~there are only a few studies on performing atmospheric correction for hyperspectral radiometer using aerosol properties retrieved from the co-located MAP measurements~~. This is ~~mostly~~ primarily due to the 15 limited availability of co-located MAP and hyperspectral radiometer measurements over ~~the ocean~~ ocean. One such dataset is available from the North Atlantic Aerosols and Marine Ecosystems Study (NAAMES) field campaign in 2015, where both the GEO-CAPE Airborne Simulator (GCAS) (a hyperspectral radiometer) and RSP were deployed. These datasets have been used to study the hyperspectral ocean color retrievals (Chowdhary et al., 2018).

In the fall of 2017, the Aerosol Characterization from Polarimeter and Lidar (ACEPOL) field campaign, a collaboration 20 between NASA and Netherlands Institute for Space Research (SRON), was conducted with six passive and active instruments on the NASA ER2 high-altitude aircraft ~~(?)~~ (Knobelgesse et al., 2020). These included four MAPs: airHARP (the airborne version of HARP2 and HARP Cubesat (McBride et al., 2019)), AirMSPI (the Airborne Multiangle SpectroPolarimetric Imager) (Diner et al., 2013), SPEX Airborne (the airborne version of SPEXone) (Smit et al., 2019) and the RSP (Research Scanning Polarimeter) (Cairns et al., 1999), and two lidars: HSRL-2 (the High Spectral Resolution Lidar-2) (Burton et al., 2015) and CPL 25 (the Cloud Physics Lidar) (McGill et al., 2002). SPEX Airborne collects hyperspectral radiometry, and thus can be used as a proxy for OCI in developing hyperspectral ocean color algorithms. The co-located MAPs and hyperspectral SPEX Airborne measurements are similar to the PACE payload, and thus provide a proxy dataset to evaluate the aerosol retrieval results from MAPs and the use of these retrieved aerosol properties for hyperspectral atmospheric correction. ~~The spectral range from the SPEX Airborne measurements used in this study is from 470 to 750 nm. This does not cover the ultraviolet (UV) bands, 30 which is nevertheless important and deems further research for the PACE mission (Frouin et al., 2019; Chowdhary et al., 2019)~~
 In this study, we build further on our previous work (Gao et al., 2018, 2019) and use the MAP measurements from RSP to 35 conduct aerosol retrievals with its well documented measurement uncertainty analysis (Knobelgesse et al., 2019), and apply the results to the atmospheric correction of the SPEX Airborne measurements. We identified two cases over the ocean from ACEPOL where SPEX Airborne measurements and Aerosol Robotic Network (AERONET) ground-based observations are collocated with RSP.

In order to retrieve aerosol information from polarimetric measurements over the ocean, a number of advanced aerosol retrieval algorithms have been developed for both airborne and spaceborne MAPs, such as POLDER/PARASOL (Hasekamp et al., 2011; Dubovik et al., 2011, 2014), AirMSPI (Xu et al., 2016, 2019), SPEX Airborne (Fu and Hasekamp, 2018; Fu et al., 2019; Fan et al., 2019), RSP (Chowdhary et al., 2005; Wu et al., 2015; Stamnes et al., 2018; Gao et al., 2018, 2019), 5 and Directional Polarimetric Camera (DPC)/GaoFen-5 (Wang et al., 2014; Li et al., 2018). In this study, we use the Multi-Angle Polarimetric Ocean coLor (MAPOL) retrieval algorithm, which is a joint aerosol and water-leaving radiance retrieval algorithm designed with the bio-optical models applicable to both open and coastal waters (Gao et al., 2018, 2019). MAP measurements from RSP include the **VIS (visible)****visible**, NIR, and SWIR **(reflectance only)****reflectance only** bands, which are used for joint aerosol and water leaving signal retrievals. The impacts of including polarization information in the retrieval of the aerosol 10 properties are studied by comparing the results with inputs of reflectance only and that of both reflectance and polarization in the MAPOL algorithm. We will also discuss the retrieval algorithm stability in terms of the sensitivity of the retrieval parameters to their initial guesses, and compare with the uncertainty estimation based on error propagation (Knobelispiesse et al., 2012). The atmospheric correction using the aerosol properties from MAP retrievals is complementary to the approaches 15 using the reflectance at NIR and/or SWIR bands to derive aerosol properties for the atmospheric correction on hyperspectral radiometers (Ibrahim et al., 2018, 2019), and is especially advantageous in scenarios where the aerosol properties in the **VIS or ultraviolet (UV) visible or UV****reflectance only** bands cannot be accurately extrapolated from measurements in the NIR-SWIR spectral range (Chowdhary et al., 2019).

The paper is organized into six sections: Sect. 2 describes the data used in the retrieval and validation of aerosol micro-physical properties and water leaving signals, Sect. 3 reviews the MAPOL retrieval algorithm and recent updates for application 20 to hyperspectral atmospheric correction, Sect. 4 and 5 present the retrieval results and discussion, and Sect. 6 summarizes the conclusions.

2 Data

During the ACEPOL field campaign, there are four flight tracks with clear skies over the AERONET USC_SEAPRISM site, located at [33.564N, 118.118W] and mounted on an oil platform roughly 18km away from the coast (Knobelispiesse et al., 2020). 25 This site is part of AERONET-OC, which uses special instruments that observe the water leaving radiance in addition to the atmospheric state (Zibordi et al., 2009). Of those four, we examined two cases in detail, as summarized in Table 1, with both RSP and SPEX Airborne measurements collocated with the AERONET measurements at the USC_SEAPRISM site. The two measurements are at the time of 2017/10/23 21:33, and 2017/10/25 21:07. Hereafter we will refer the two cases as Case 10/23 and Case 10/25. The locations and viewing geometries for both RSP and SPEX are specified in Fig. 2-1. Case 10/23 is close to 30 the principal plane with a relative azimuth angle of 8.7°; while Case 10/25 is almost perpendicular to the principal plane with a relative azimuth angle of 94.6°. The two cases have similar solar zenith angles of 53.3° and 50.9°.

RSP is the airborne version of the Aerosol Polarimetry Sensor for the NASA Glory mission that has been flown in multiple field campaigns since 1999 (Cairns et al., 1999). It is a multi-angle scanner measuring 152 viewing angles within

60° fore and aft of nadir in the along track direction, in 9 channels from [VIS-visible](#) to SWIR (center wavelengths 410, 470, 555, 550, 670, 865, 960, 1590, 1880, 2250 nm). SPEX Airborne is a hyperspectral imager with the spectral range of 400-800 nm. Its spectral resolution is 10-20 nm for degree of polarization (DoLP) and 2-3 nm for intensity. SPEX Airborne has 9 viewing angles (different from the 5 viewing angles of SPEXone) within the angular range of 112°($\pm 56^\circ$). The SPEX measurements with wavelengths larger than 750 nm are excluded from our analysis due to a grating order overlap issue in the data (Smit et al., 2019; Fu et al., 2019). The RSP and SPEX Airborne data files used in this study are listed in the Data Availability section.

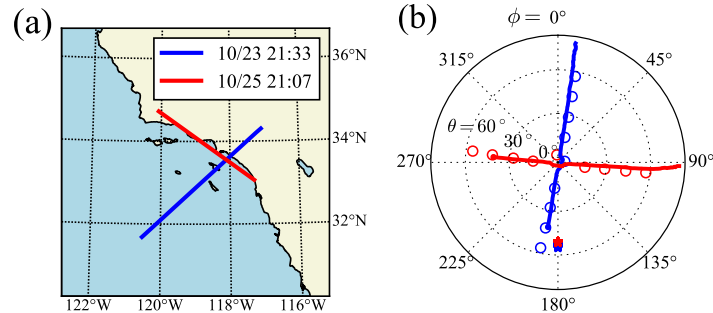


Figure 1. (a) The flight tracks across the AERONET USC_SEAPRISM site. The legend shows the time at which the aircraft flew over the AERONET site. (b) The corresponding polar plot for the RSP (solid line) and SPEX (open circles) viewing directions as summarized in Table 1, where θ is the zenith angle, and ϕ is the relative to azimuth angle between the solar direction indicated by asterisk symbols instrument viewing azimuth angle and the sunlight azimuth angle. Aircraft crossing time for The asterisk symbol indicate the AERONET site is indicated in the legend antisolar point.

Table 1. Summary of the datasets from ACEPOL field campaigns used in this study.

Date	2017/10/23	2017/10/25
UTC Time	21:33	21:07
Distance to AERONET site	1.6 km	1.2 km
Aircraft altitude	20.1 km	19.7 km
Solar zenith angle	53.3°	50.9°
RSP relative azimuth angle	8.7°	94.6°
RSP scattering angle range	[113.9°, 166.9°]	[108.5°, 129.7°]
Solar zenith 53.3° 50.9° Relative azimuth 8.7° 94.6° Aircraft altitude 20.1 km 19.7 km height		

To validate the aerosol retrieval results, we will compare our retrieved aerosol properties with the aerosol products from HSRL-2 and AERONET. The HSRL instruments provide accurate assessment of AOD at 355 and 532 nm (Hair et al., 2008). In this study, the [HSRL-2](#) AOD product at 532 nm from the ACEPOL campaign with an assumed Lidar ratio is used. The AERONET USC_SEAPRISM site is equipped with a CIMEL based system called the Sea-Viewing Wide Field-of-View Sensor

(SeaWiFS) Photometer Revision for Incident Surface Measurements (SeaPRISM), at eight wavelengths of 412, 443, 490, 532, 551, 550, 667, 870, and 1020 nm with a bandwidth of 10 nm (Zibordi et al., 2009). The AERONET instrument provides direct Sun and diffuse sky-radiance measurements to infer aerosol properties (Holben et al., 1998). The measurements of direct Sun radiation are used to derive the spectral AOD with an uncertainty of (Holben et al., 1998; Eck et al., 1999; Holben et al., 2001; Smirnov et al., 2000).

5 The AERONET Version 3 Level 2.0 data are used in this study, where the estimated AOD uncertainty is from 0.01 for mid-visible wavelengths and to 0.02 for UV wavelengths (Holben et al., 1998; Eck et al., 1999; Holben et al., 2001; Smirnov et al., 2000) with the maximum uncertainty in the UV channels (Giles et al., 2019). The diffuse sky-radiance measured at a wide range of scattering directions is used to infer aerosol size, complex refractive index and non-spherical particle ratio (Dubovik and King, 2000; Dubovik et al., 2006). For AOD less than 0.2, uncertainties in the AERONET inversion products are estimated as 10 15–35% for size distribution depending on aerosol types, 0.05 for refractive index and 0.05–0.07 for single scattering albedo (SSA) (Dubovik et al., 2000). The AERONET measurement capability can be extended to include photopolarimetric measurement with the next-generation Sun photometer, and its improvement on aerosol property retrievals has been demonstrated (Xu and Wang, 2015; Xu et al., 2015; Fedarenko et al., 2016), although such retrievals were not available for this study.

The retrieved ocean color results are compared to AERONET Ocean Color (AERONET-OC) and the Moderate Resolution Imaging Spectroradiometer Ocean Color (MODIS OC) products. The MODIS OC product is processed with the atmospheric correction algorithm originating from Gordon and Wang (Gordon and Wang, 1994; Mobley et al., 2016) with the aerosol model from Ahmad et al. (Ahmad et al., 2010) and is publicly available (NASA Ocean Color Web). MODIS OC provides a spatial coverage with 1km resolution at nadir. Since the aerosol properties and water leaving signals are measured or derived at different times, geometries and spatial resolutions, natural variation is a factor contributing to the difference when comparing 20 the retrieved results. In order to evaluate the spatial variations when comparing with the retrieved water leaving reflectance, we averaged the MODIS (on board Aqua) water leaving reflectance within a 2km region around the USC_SEAPRISM site and compute its standard deviation as its maximum uncertainty. If smaller than 5%, the uncertainty is adopted as 5% which is the accuracy goal for blue band and clear water (Hu et al., 2013). The AERONET measurements are available in almost every hour and there are a total of 8 measurements each day. Therefore, the The AERONET product provides good temporal 25 coverage of the aerosol and ocean reflectance. We averaged the one-day AERONET products and compared both its mean and variability its mean with the retrieval results, where the standard deviation (6% to 10% for both cases) is used to represent the uncertainties. The reported uncertainty for AERONET OC R_{rs} is approximately 5% between 410–550 nm (Zibordi et al., 2009). Note that the actual inversion uncertainties for the aerosol properties, such as the refractive index and single scattering albedo (SSA), may be larger than their daily averaged result for small AOD cases as reported by the AERONET Version 3 30 uncertainty analysis (Description of Aerosol Inversion Uncertainty for Level 2 Products). In general, AERONET retrievals of aerosol microphysical properties become less certain as AOD decreases.

The AODs for the two cases in our discussion are around 0.03~0.04 at around 550 nm, as reported by HSRL-2 and AERONET observations. It is challenging to retrieve aerosol micro-physical properties when the aerosol loading is small. Meanwhile the water leaving signals are often represented by the remote sensing reflectance (R_{rs} ; sr^{-1}) as a ratio of the 35 upwelling radiance and downwelling irradiance both just above the ocean surface (Mobley et al., 2016). In this study R_{rs}

is also small with a value around 0.002-0.003 sr^{-1} from 400- 550 nm reported by the AERONET Ocean Color product, which account for 5% to 15% of the total signal measured at the aircraft level. The percentage contribution of the water leaving ~~reflectance signals~~ to the observations depends on the polarization state and the water conditions (Zhai et al., 2017) (Chowdhary et al., 2012; Zhai et al., 2017). Although the aerosol loading is small, its contribution is of the same order of magnitude as the ~~contribution of the~~ water leaving signal ~~contribution~~ between 400-550 nm range, and hence remains important for atmospheric correction. Therefore, both the retrieval of aerosol micro-physical properties and the water leaving signals require high accuracy of the measurements from RSP and SPEX Airborne.

Smit et al. provided a thorough comparison of the reflectance and polarization measurements between SPEX Airborne and RSP from ACEPOL over ocean, cloud and land scenes (Smit et al., 2019). For the ocean scenes, eight flight tracks were selected, and both the random and systematic difference between the two sensors were analyzed. Over the four RSP bands of 410, 470, 550, 670 nm, the random noise contribution to differences of ~~reflectances~~ ~~reflectance~~ are 2%, 2%, 2% and 4%. ~~The systematic differences are larger than the random differences RSP reflectance is slightly larger than SPEX reflectance at 410 and 470 nm, which are as indicated by their systematic differences of around 4% and 3% respectively, larger than the random differences; the systematic differences at the other two bands are relatively small with values of 0% and 1%.~~ For DoLP, the random differences are 0.007, 0.005, 0.003, and 0.008 for the four bands from 410 to 670 nm; and systematic differences are either similar or smaller. This suggests that DoLP differences are dominated by random errors, while reflectances show systematic difference larger than the random noise at 410 and 470 nm. The systematic difference in reflectance also poses challenges in atmospheric correction for SPEX Airborne in the wavelengths between 410 and 470 nm. Polarization information shows a higher level of agreement between the two sensors and therefore should be more strongly weighted in the retrieval algorithm.

3 Method

The MAPOL algorithm is designed to jointly retrieve the aerosol and water leaving signals from MAP data, which has been validated with the synthetic simulated data (Gao et al., 2018) as well as the RSP measurements from field campaigns (Gao et al., 2019). The retrieval algorithm minimizes the difference between the MAP measurements and the forward model simulations computed from a vector radiative transfer forward model (Zhai et al., 2009, 2010). Two ocean bio-optical models are implemented in MAPOL: one with Chlorophyll-a concentration as the single retrieval parameter applicable to open ocean optical properties, and the other with seven parameters applicable to complex coastal waters (Gao et al., 2019). In this study we perform retrievals near the USC_SEAPRISM site where waters are mostly clear so that the bio-optical model parameterized by Chlorophyll-a concentration is used.

In the MAPOL algorithm used in this study, the aerosol size distribution is composed by five sub-modes, each with a lognormal distribution with fixed mean radius and variance (Dubovik et al., 2006; Xu et al., 2016, 2017). The first three sub-modes (median radii of 0.1, 0.1732, 0.3 μm) represent the fine mode aerosols, and the last two sub-modes (median radii of 1.0, 2.9 μm) represents the coarse mode aerosols. For a general study, Fu et al. and Hasekamp discussed the representation of

aerosol size distribution through various numbers of sub-modes and found that similar five mode approach can provide good retrievals for most aerosol parameters (Fu and Hasekamp, 2018). The aerosol refractive index spectra for both fine and coarse modes are approximated as $m(\lambda) = m_0 + \alpha_1 p_1(\lambda)$, where m_0 and α_1 are fitting parameters, and $p_1(\lambda)$ is the first order of the principal components, computed from the dataset derived from Shettle and Fenn (1979), including spectral refractive indices 5 of water, dust-like, biomass, industrial, soot, sulfate, water soluble and sea salt aerosols (d'Almeida et al., 1991; Wu et al., 2015). There are two sets of m_0 and α_1 for the real and imaginary refractive index spectra, respectively, for both the fine and coarse modes. This means that there are a total of 8 parameters for the refractive indices. In summary, the retrieval parameters 10 include 5 volume densities (one for each sub-mode), 8 parameters for the refractive indices of fine and coarse modes, one parameter for wind speed, and the Chlorophyll-a concentration, with a total of 15 parameters. After the aerosol properties are retrieved from the discrete bands of the RSP data, the same parameters m_0 and α_1 are used in the aforementioned refractive index spectral representation to calculate the aerosol refractive indices at the SPEX Airborne wavelengths, which are then used 15 in the radiative transfer model to compute the contribution of aerosols at the corresponding wavelengths.

The Stokes parameters, L_t , Q_t , and U_t , from RSP measurements are used to define the total measured reflectance $\rho_t = (\pi r^2 L_t) / (\mu_0 F_0)$ and total DoLP $P_t = \sqrt{Q_t^2 + U_t^2} / L_t$ where F_0 is the extraterrestrial solar irradiance, μ_0 is the cosine of solar 15 zenith angle, r is the Sun-Earth distance in astronomical units. Circular polarization (Stokes parameter V), not measured by any of the polarimeters in ACEPOL, is often ignored for atmospheric studies (Kawata, 1978). The cost function is used to quantify the difference between the measurement and the forward model simulation and is defined as:

$$\chi^2(\mathbf{x}) = \frac{1}{N} \sum_i \left(\frac{[\rho_t(i) - \rho_t^f(\mathbf{x}; i)]^2}{\sigma_t^2(i)} + \frac{[P_t(i) - P_t^f(\mathbf{x}; i)]^2}{\sigma_P^2(i)} \right) \quad (1)$$

where ρ_t^f and P_t^f denotes the total reflectance and DoLP simulated from the forward model; the state vector \mathbf{x} contains 20 retrieval parameters for aerosols and ocean; subscript i stands for the indices of the measurements at different viewing angles and wavelengths; and N is the total number of the measurements used in the retrieval. All RSP bands are used in our retrievals except for the two water vapor absorption bands at 960 nm and 1880 nm. The total uncertainties of the reflectance and DoLP used in the algorithm are denoted as σ_t and σ_P , which includes three components: the instrument measurement uncertainties 25 as summarized in Knobelgesse et al. (2019) (e.g. absolute radiometric and ~~polarimetric characterization~~ DoLP uncertainty averaged to ~~0.03-3%~~ and 0.002 for the RSP instrument used in ACEPOL), the variance from averaging nearby RSP pixels (the average of 5 consecutive pixels are used in this study, which corresponds to a surface pixel size of approximately 1km), and the forward model uncertainties estimated as 0.015 and 0.002 for the radiometric and polarimetric uncertainties, respectively (Gao et al., 2019). All these ~~uncertainties~~ are added in the quadrature of σ_t and σ_P in Eq. 1 to represent the total 30 uncertainties. The weight of the measurements in the cost function depends on the inverse square of σ_t and σ_P . As will be discussed shortly, there are higher weight on the DoLP than reflectance in the cost function. Because DoLP has less dependency on the noise correlation between angles due to its definition as a ratio of two observations (Knobelgesse et al., 2012), the noise correlation has been ignored in this study.

The relative uncertainties for reflectance and DoLP, denoted as σ_t / ρ_t and σ_P / P_t , are defined as the ratio of the total uncertainties over the measurement, and summarized in Table 2. The magnitude of uncertainties often depends on the viewing angles

as shown in the panels (c) and (d) of Figure 2 and 3. Table 2 shows the minimum value among the viewing angles at each band which corresponds the largest weight in Eq. 1 for the corresponding band. The value of σ_t/ρ_t is 3.4% from 410 nm to 865 nm, and around 4% to 5% for the SWIR bands. σ_P/P_t is between 0.4% to 1.8% for the bands from 410 nm to 865 nm, and for the SWIR bands, σ_P/P_t is between 6.1% to 15.1%. The percentage uncertainties of the polarizations in the two SWIR bands 5 further ~~increases~~ increase when the DoLP value decreases. We have tested the effects of the DoLP at the two SWIR bands on the aerosol retrieval and found that including them does not improve the retrieval accuracies, so the SWIR DoLPs are not used in our retrievals. Moreover, the PACE MAPs do not include polarimetric SWIR measurements ~~so the SWIR DoLPs are not used in our~~ but PACE OCI includes several SWIR bands measured at a single viewing angle and may have higher accuracy, a 10 synergy of PACE OCI SWIR with MAP measurements may further improve aerosol retrievals. In summary we use seven bands of ρ_t and five bands of P_t in our retrievals, and the corresponding cost function is denoted as $7\rho_t + 5P_t$. In order to understand the impacts of the polarization information, we also conducted the retrievals with only reflectance in the cost function which is denoted as $7\rho_t$.

Table 2. The minimum relative uncertainties of reflectance (ρ_t) and DoLP (P_t) for the RSP bands. The SWIR DoLPs denoted by asterisks are not used in the retrievals.

Cases	Wavelength(nm)	410	470	550	670	865	1590	2250
10/23	σ_t/ρ_t (%)	3.4	3.4	3.4	3.4	3.4	3.9	4.7
	σ_P/P_t (%)	0.5	0.5	0.7	1.0	1.8	8.5*	15.1*
10/25	σ_t/ρ_t (%)	3.4	3.4	3.4	3.4	3.4	3.7	4.8
	σ_P/P_t (%)	0.4	0.4	0.5	0.6	1.1	6.1*	14.5*

The use of oceanic sun glint from satellite measurements has been proposed and demonstrated to help aerosol absorption retrievals (Kaufman et al., 2002; Ottaviani et al., 2013). However, we tested the retrievals with the sun glint data included for 15 Case 10/23 (as shown in Fig. 2) and found that the sun glint reflection cannot be modelled well using the isotropic Cox-Munk model (Cox and Munk, 1954) which depends on the wind speed only. This may be due to the high spatial resolution of 200m from RSP measurement or the insufficient representation with a scalar wind speed. Therefore, the sun glint region for only Case 10/23 is removed within an angle of 40° around the specular reflection direction of the direct solar light as indicated in Figure 3. There is no data removed by the glint mask for Case 10/25 due to its cross-principal plane geometry. The remaining 20 range of scattering angles used in the retrieval are shown in Table 1.

The retrieved aerosol properties will be compared and validated with the AERONET products in the next section, and then used to conduct atmospheric correction for both RSP and SPEX airborne measurement. The resultant water leaving signals as represented by the remote sensing reflectance can be computed using the water leaving reflectance reaching the sensor ρ_w^{Sensor} as ρ_w^{Sensor} as

$$25 \quad R_{rs} = \rho_w^{Sensor}/(\pi r^2 t_d t_u) \quad (2)$$

where t_d is the downward transmittance of the solar irradiance to the surface, and t_u is the upward transmittance of the water leaving radiance to the sensor(Gao et al., 2019). The water leaving reflectance ρ_w^{Sensor} represents the water leaving signals originating from scattering in the ocean and reached the sensor, and can be derived from the atmospheric correction process by subtracting as

$$5 \quad \rho_w^{Sensor} \equiv \rho_t - \rho_{t,atms+sfc}^{Sensor} \quad (3)$$

where $\rho_{t,atms+sfc}^{Sensor}$ is the reflectance contribution of atmosphere and ocean surface from the measurement at the aircraft (Gao et al., 2019) at the sensor (Mobley et al., 2016; Gao et al., 2019). In order to compare the water leaving signals measured at different times derived from RSP, MODIS and AERONET instruments, the directional dependence of the water leaving reflectance is removed to obtain the signal at the nadir direction (Mobley et al., 2016).

10 After obtaining the aerosol properties from RSP retrievals, the atmospheric contributions including all the scattering and absorption process related to the aerosols, molecules and ocean surface, and the t_d and t_u transmittance are computed for the hyperspectral SPEX spectral bands with the vector radiative transfer model by Zhai et al. (Zhai et al., 2009, 2010, 2018) and subtracted from the hyperspectral SPEX Airborne measurement. The gas absorption in the radiative transfer simulation, including contributions from ozone, oxygen, water vapor, nitrogen dioxide, methane, and carbon dioxide, are accounted by using the
15 US standard atmospheric constituent profiles (Anderson et al., 1986) but with scaled amount of water vapor, ozone and oxygen. The total ozone column density used to scale the ozone profile is obtained from the Modern-Era Retrospective analysis for Research and Applications, Version 2 (MERRA-2) from NASA's Global Modeling and Assimilation Office (Gelaro et al., 2017).
20 The total We then simulated the reflectance spectra under SPEX geometries with the retrieved aerosol properties and various amounts of oxygen and water vapor. The simulated spectra are compared with SPEX Airborne measurement, and the best amounts of water vapor and oxygen are computed from minimizing chosen to minimize the difference between measurement and simulated SPEX Airborne measurement over all the bands the measurements and simulations. During this process the aerosol properties and ozone density are kept unchanged. The hyperspectral variations of gas absorption are incorporated in the radiative transfer simulation using a method similar to the double-k method (Zhai et al., 2018).

4 Results

25 The MAPOL retrieval algorithm was applied to the RSP measurements for the Cases 10/23 and 10/25. To evaluate the retrieval stability and uncertainties, 150 sets of random initial guesses for all the 15 retrieval parameters were used for the cost functions of both $7\rho_t + 5P_t$ and $7\rho_t$. Each parameter was varied within a boundary as specified in Gao et al. (2018),
(Gao et al., 2018, 2019), where the wind speed is less than 10 m/s and the Chlorophyll a concentration is less than 30 mg/m³,
the aerosol refractive index varies effectively between 1.3 to 1.6 in its real part, and between 0 to 0.03 in its imaginary part,
30 and random mixing fractions of the five aerosol volume densities constrained by a maximum total AOD of 0.3. The minimum cost function value χ_{min}^2 for Case 10/23 and 10/25 are 2.8 and 3.8 with the cost function of $7\rho_t + 5P_t$ and reduced to 0.6 and 0.4 with the cost function of $7\rho_t$ (polarization information not considered, all else the same). The minimum cost function value

corresponds to the best aerosol retrievals, and the remaining residuals relate to the measurements which cannot be completely represented by the forward models.

Using the best aerosol retrievals corresponding to χ^2_{min} for $7\rho_t + 5P_t$, the reflectance and DoLP are simulated and compared with the measurements as shown in Fig. 2 and Fig. 3. The positive, where the viewing zenith angles refer to the viewing angles on the glint side are the same as defined in Fig. 1(b) with the positive sign referring to the glint side ($\phi < 90^\circ$ or $\phi > 270^\circ$), and the negative viewing zenith angles refer to the sun side sign referring to the other hemisphere containing the antisolar point. The solid line is for indicates the measurement data and the dashed line is indicates the simulation results using the retrieved aerosol and ocean properties for the reflectance (ρ_t) and DoLP (P_t) as plotted in panels (a) and (b). The total uncertainties as discussed in Section 2 are plotted in panels (c) and (d) for the reflectance and DoLP respectively. The percentage difference between measurements and fittings is plotted in panels (e) and (f). For Case 10/23, the viewing directions are close to the principal plane. The sun glint is indicated by the shaded area in Figs. 2, which were excluded in the retrieval as discussed in Section 3. Using the retrieved aerosol properties, the reflectance and DoLP were also computed in the glint region. Although both the reflectance and DoLP measurements in the glint region were not considered in this study, the comparison of the measurement and simulated results indicates a better agreement of the DoLP than the reflectance, which can be explained by the fact that the DoLP from reflection on the ocean surface does not depend on the assumed distribution of surface slopes. For the remaining angles, the absolute residual larger than 10% in Figs. 2(c) and 2(d) are mostly associated with the small values of the measurement, such as the SWIR bands for ρ_t , and the DoLP at viewing angles less than -20° . On average, the residual for both reflectance and DoLP are smaller than 6%. For Case 10/25, the viewing angles are almost perpendicular to the principal plane, the DoLP is always larger than 0.3, and the residuals for DoLP are even smaller than previous case with a value less than 2% on average. For the SWIR bands at the viewing angles between -10° and 20° , Fig 3(e) shows residuals larger than 10% at 1590 nm and 2250 nm, which indicates the measurements cannot be modelled by the forward model. However, the difference is not observed in the DoLP comparisons in Fig. 3(f). Due to the presence of invalid measurements in the 2250 nm band between -10° and 20° , some measurement uncertainties in this portion are not computed as shown in Fig 3(c) and the corresponding measurements are not counted in the cost function.

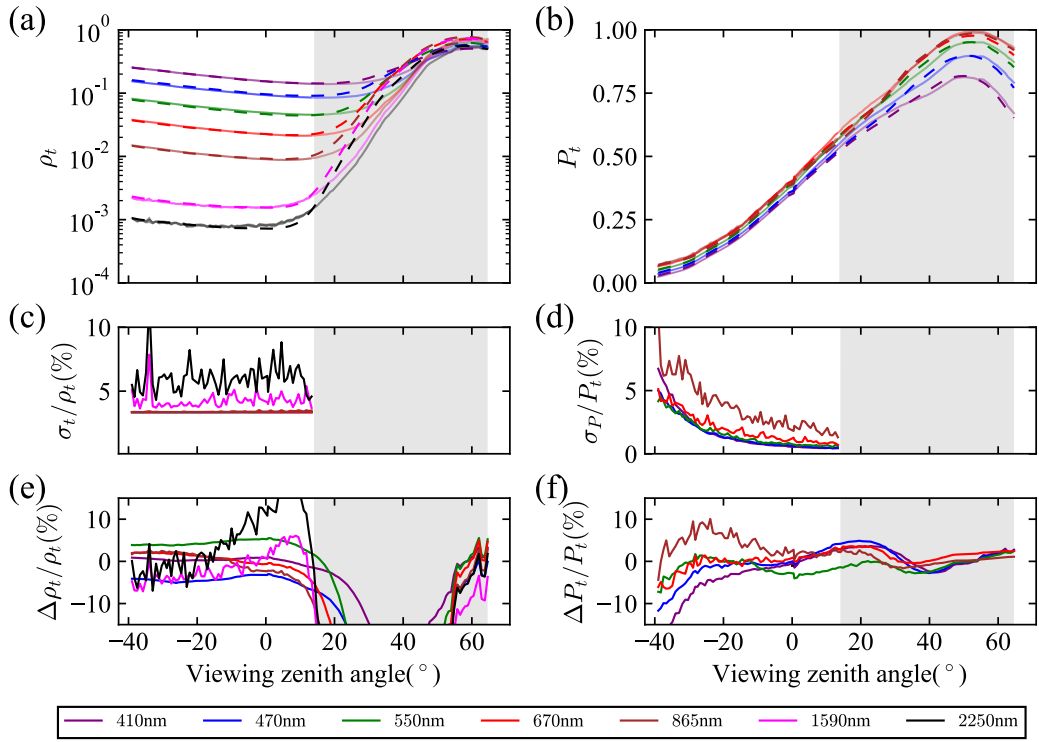


Figure 2. (a) and (b) The comparison of the RSP measurement and model fitting of reflectance ρ_t and DoLP P_t for Case 10/23, (c) and (d) are the total percentage uncertainties relative to the measurements for reflectance ($100\sigma_t / \rho_t$) and DoLP ($100\sigma_P / P_t$), (e) and (f) are the percentage residuals between the measurements and fittings relative to the measurements for reflectance ($100\Delta\rho_t / \rho_t$) and DoLP ($100\Delta P_t / P_t$). The solid line in (a) and (b) is the measurement data and the dashed line is the simulation results from the retrieval. The shaded area indicates the angles not used in the retrieval (uncertainties are not calculated).

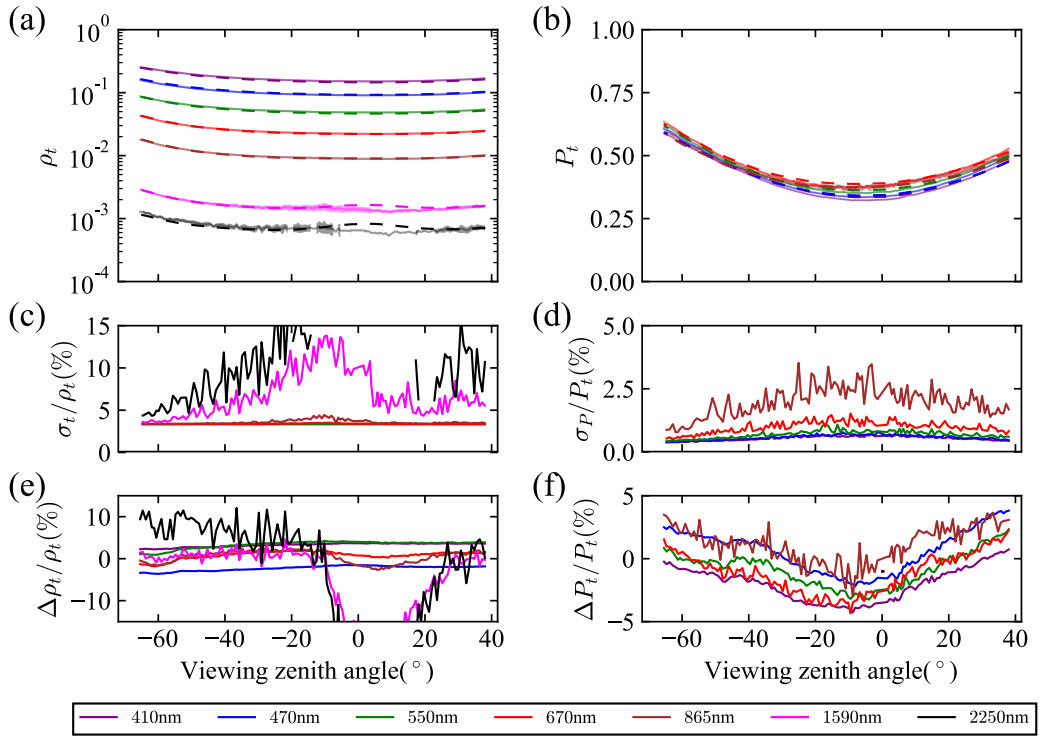


Figure 3. Same as Fig. 2 but for Case 10/25.

The histogram and cumulative probability of the cost functions for the 150 converged cases with random initial values are compared in Fig. 4. For the cost function $7\rho_t$ more than 50% cases are converged within a cost function value of 2 (the residual is $\sqrt{2}$ times the measurement uncertainty), while to have the same 50% cases converged for $7\rho_t + 5P_t$, the cost function value needs to be within 6. The wider spread of the cost function values is related to the higher sensitivity of DoLP in the 5 cost function, which is consistent with Table 2 showing that the DoLP has much smaller uncertainties. In order to evaluate the uncertainties of the best retrieval results, we consider the retrieval cases to be converged within a cut-off cost function value of $\chi_{min}^2 + 1$, and compute the standard deviation of all the aerosol properties and water leaving signals retrieved from these cases. This corresponds to the evaluation using all the retrieval cases converged within the cost function range of $[\chi_{min}^2, \chi_{min}^2 + 1]$. There are 50% of the retrievals in average converged within this cost function range for $7\rho_t$, while 30% of all the retrievals 10 converged within this requirement for $7\rho_t + 5P_t$. More discussion on the cut-off cost function value is in the next section. A comparison of the results with 75 and 150 cases demonstrated that the results are converged with enough samples to compute the standard deviation. The uncertainties due to the impact of the initial values is addition to the uncertainties from the error propagation method, where the measurement uncertainties are propagated to the retrieval parameters through the Jacobian matrix (e.g. Knobelspiesse et al. (2012)). A further discussion in the next section suggests that the uncertainties evaluated 15 using these two methods may also ~~related~~relate to each other.

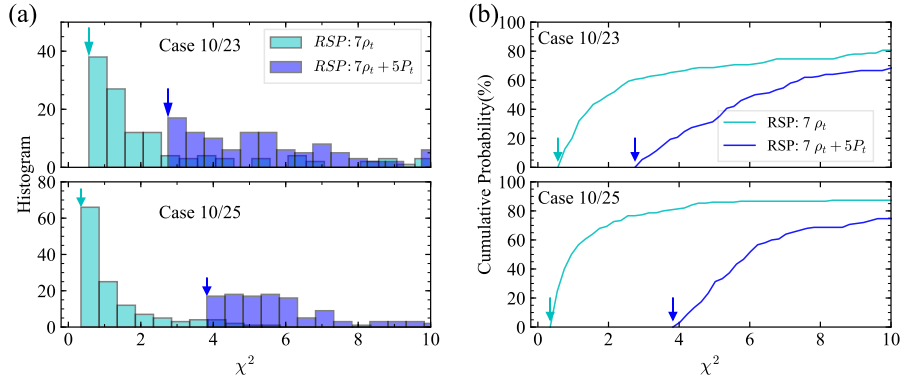


Figure 4. (a) The histogram for Case 10/23 and 10/25 with cost function $7\rho_t$ and $7\rho_t + 5P_t$ and a bin size of 0.5; (b) the corresponding cumulative probability. The arrows indicate the minimum cost function values χ^2_{\min} .

4.1 Aerosol micro-physical properties

We compared the retrieved aerosol size distribution, fine mode refractive index, fine mode SSA and total AOD with the averaged AERONET product on the same day in Fig. 5. The aerosol size distribution is represented by the volume density as a function of radius in the logarithmic scale. Both the shaded area and the error bar indicate 1-sigma uncertainty. The retrieval values and uncertainties are summarized in Table 3, which includes wind speed, refractive index and SSA spectra, SSA and AOD for both fine and coarse modes, and remote sensing reflectance. The overall SSA for the two mode mixture is computed as the ratio of the number density weighted averages for the scattering and extinction cross sections (Bohren and Huffman, 1998). For Case 10/23, the retrieved wind speed for both cost functions are $3.4 \sim 3.5 \text{ m/s}$ with similar uncertainties. For 10/25, a wind speed of 5.4 m/s is retrieved under $7\rho_t + 5P_t$ which is 1.5 m/s faster than the results from $7\rho_t$ and with the uncertainty reduced by a factor of 2. Due to the exclusion of the glint in the retrieval for Case 10/23 and the cross principal plane geometry for Case 10/25, the wind speed is not ideal for retrieval. However, the retrieval uncertainties are within 0.5 m/s for both cases with $7\rho_t + 5P_t$, which suggests that the measurements used in the retrievals are still influenced by wind speed.

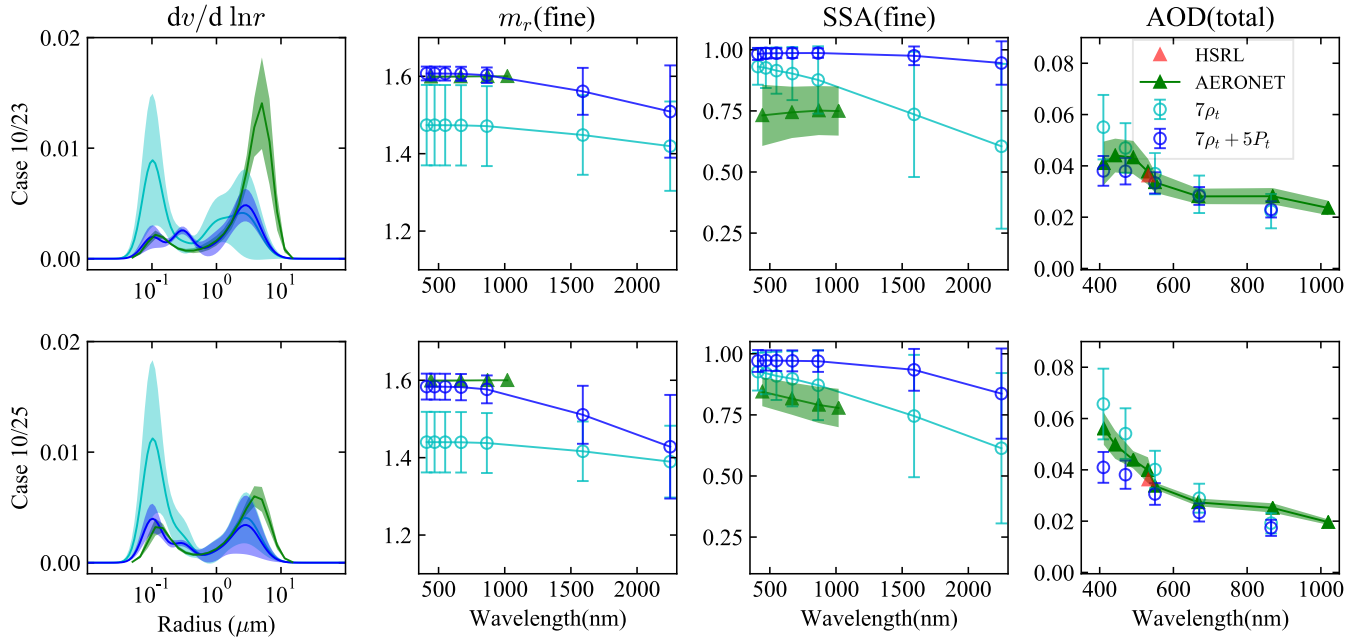


Figure 5. The aerosol size distribution ($dv/d \ln r$), fine mode refractive index(m_r), fine mode SSA, and total AOD of the two cases on 10/23 and 10/25 retrieved with the cost functions of $7\rho_t + 5P_t$ and $7\rho_t$. The vertical widths for the aerosol size distribution and the error bars for other aerosol properties of the retrieved results indicates indicate one sigma retrieval uncertainties. The results from AERONET product are plotted in green, and the vertical width indicates its daily variation. The HSRL AOD at 532 nm is indicated by the red triangle.

Table 3. The averaged retrieval values and uncertainties(in [parenthesis](#)) from the cases converged within the range of cost function $[\chi^2_{min}, \chi^2_{min} + 1]$ for fine and coarse mode effective radius (r_{eff}), effective variance (v_{eff}), refractive index (m_r), SSA, as well as total AOD and SSA, and remote sensing reflectance (R_{rs}). AOD, SSA and m_r are all at 550 nm, and R_{rs} is at both 470 and 550 nm.

Date	10/23	10/23	10/25	10/25
Cost Function	$7\rho_t$	$7\rho_t + 5P_t$	$7\rho_t$	$7\rho_t + 5P_t$
Wind Speed(m/s)	3.48(0.26)	3.42(0.34)	3.91(1.18)	5.42(0.49)
r_{eff} (fine)(μm)	0.12(0.03)	0.16(0.03)	0.12(0.03)	0.12(0.01)
v_{eff} (fine)	0.26(0.11)	0.45(0.08)	0.28(0.09)	0.41(0.05)
m_r (fine)	1.47(0.10)	1.61(0.02)	1.44(0.08)	1.58(0.03)
SSA(fine)	0.91(0.09)	0.99(0.02)	0.91(0.10)	0.97(0.04)
AOD(fine)	0.025(0.005)	0.027(0.004)	0.035(0.007)	0.026(0.003)
r_{eff} (coarse)(μm)	1.60(0.45)	1.78(0.42)	2.07(0.47)	1.70(0.52)
v_{eff} (coarse)	0.58(0.13)	0.54(0.13)	0.44(0.14)	0.52(0.15)
m_r (coarse)	1.52(0.12)	1.56(0.11)	1.57(0.10)	1.53(0.11)
SSA(coarse)	0.68(0.03)	0.65(0.04)	0.75(0.16)	0.79(0.14)
SSA AOD(coarse)	0.012 (total)0.007	0.006(0.003)	0.005(0.003)	0.005(0.003)
SSA (overall)	0.84(0.07)	0.92(0.03)	0.89(0.09)	0.94(0.04)
AOD(total)	0.037(0.008)	0.033(0.004)	0.040(0.007)	0.031(0.004)
R_{rs} (470nm 470 nm)(sr^{-1})	0.0027(0.0003)	0.0026(0.0003)	0.0024(0.0004)	0.0025(0.0003)
R_{rs} (550nm 550 nm)(sr^{-1})	0.0021(0.0001)	0.0020(0.0002)	0.0020(0.0002)	0.0021(0.0001)

Fig. 5 shows that the aerosol size distribution retrieved with the polarized information $7\rho_t + 5P_t$ is closer to the AERONET results than that of the reflectance only retrieval ($7\rho_t$): the the maximum fine mode volume density reduced by 4 and 2.5 times for Case 10/23 and 10/25, and the uncertainties reduced by five times for both cases. The fine mode effective radii of $7\rho_t$ and $7\rho_t + 5P_t$ are similar for each, but the effective variances become larger when DoLP observations are included with an increase of around 0.1 to 0.2, as shown in Table 3. An increase of the fine mode effective variances can also be observed in Fig. 5 with a wider fine mode distribution. To compensate the much smaller fine mode density from the retrievals with $7\rho_t + 5P_t$, the retrieved fine mode refractive indices increase from 1.47 to 1.61 and from 1.44 to 1.58, for Cases 10/23 and 10/25 respectively. [To compare with the AERONET results which assume that both fine and coarse modes have the same refractive index, we define the volume-averaged refractive index as \$m_v = f_v \times m_r\$ \(fine\)+\(1 - \$f_v\$ \) \$\times m_r\$ \(coarse\) where \$f_v\$ is the fine mode volume fraction \(Hasekamp et al., 2011; Gao et al., 2018\).](#) For Cases 10/23 and 10/25 with $7\rho_t$, [which agree](#) m_v is 1.49 and 1.48 respectively. While with $7\rho_t + 5P_t$ m_v becomes 1.58 and 1.56 for these two days which [agrees](#) better with the AERONET [results](#) refractive index of 1.6.

Meanwhile, a larger fine mode SSA is also retrieved with the polarization information (from 0.91 to 0.99 for Case 10/23 and from 0.91 to 0.97 for Case 10/25) which suggests the aerosols have almost no absorption. The coarse mode SSAs are of 0.7 ~ 0.8 for both days and both cost function options. [Moreover, including polarization in the retrievals, the uncertainties for](#)

refractive index, SSA and AOD become $0.02 \sim 0.03$ for refractive index, $0.02 \sim 0.04$ for SSA, and 0.004 for AOD, which are reduced nearly by one half.

The AERONET SSAs at 550 nm are around 0.8 (with a daily variation of 0.1), which are smaller than the retrieved ~~total SSA~~ ~~overall SSA at 550nm~~ with a value of 0.92 for Case 10/23 and 0.94 for Case 10/25 with $7\rho_t + 5P_t$. ~~The coarse mode SSAs are similar for both cost functions around 0.7 and 0.8 respectively, while the fine mode in RSP retrievals shows much less absorption. The HSRL AOD at 532 nm, and the mean AERONET AOD at 550 nm are the same for~~ ~~For AOD comparisons, the HSRL AODs are 0.036 at 532 nm for both Case 10/23 and 10/25 with a value of 0.036 and 0.034 respectively, which agrees with the AERONET AODs at the same wavelength are 0.038 and 0.040 respectively, and become 0.034 at 550 nm. These AOD results agree~~ well with the retrieved AODs ~~at 550 nm~~ (0.033 for Case 10/23 and 0.031 for Case 10/25). The AERONET AOD spectra are in good agreement with the RSP AOD spectra in terms of both shape and magnitude for Case 10/23, but are slightly larger than that of Case 10/25 with a difference of 0.011 at 410 nm. ~~Note that AERONET aerosol product uncertainties are approximately 0.01 for AOD, 0.05 for~~

~~When including polarization in the retrievals, the fine mode retrieval uncertainties become $0.02 \sim 0.03$ for refractive index, $0.02 \sim 0.04$ for SSA, and $0.05 \sim 0.07$ for SSA as mentioned in Section 2, which are comparable with the results for $7\rho_t$ but larger than the ones from $7\rho_t + 5P_t$. The differences between the AERONET aerosol product and aerosol retrievals with $7\rho_t + 5P_t$ are mostly within the uncertainty range 0.004 for AOD, with most values reduced by more than one half. The uncertainties for most coarse mode properties remain with similar magnitudes. However, the aerosol signals are small due to the small AOD and small aerosol signals in our cases~~ can be easily influenced by other environmental factors not modeled by the forward model, more case studies are required to evaluate the overall agreement and bias.

20 4.2 Water leaving reflectance

The aerosol properties retrieved with the best fit results using $7\rho_t + 5P_t$ were applied to the atmospheric correction of the hyperspectral measurements from SPEX Airborne for both Case 10/23 and 10/25 using the methods discussed in Section 3. The retrieval uncertainties of the water leaving reflectance for the RSP R_{rs} were computed similarly to that for the aerosol properties. The results are compared with the ~~in-situ MODIS OC products and the SeaPRISM~~ measurements from AERONET ~~OC and MODIS OC products~~ in Fig.6. The AERONET and MODIS OC agree well with each other for Case 10/25; for Case 10/23 MODIS R_{rs} is lower than AERONET R_{rs} by a value of 0.001 sr^{-1} at 470 nm. The uncertainties from MODIS OC and AERONET OC data as defined in Section 2 are smaller than the RSP retrieval results, which indicate the small temporal and spatial variations of the water leaving reflectance, and therefore their results can be used to compare with the RSP retrievals at a slightly different time and location (Table 1).

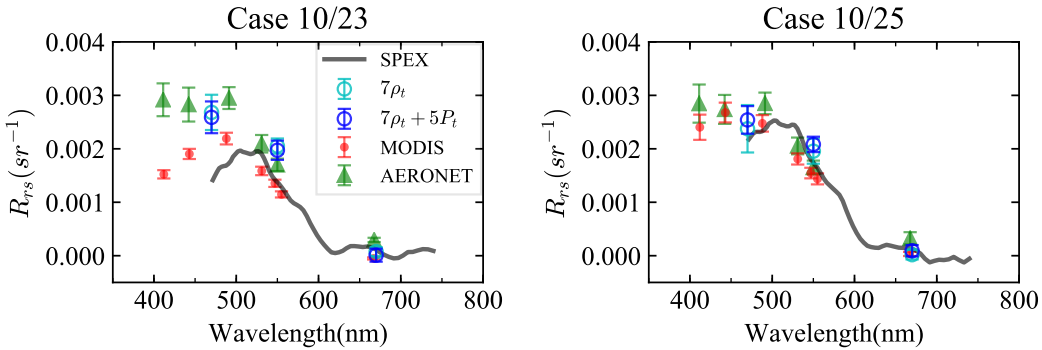


Figure 6. The remote sensing reflectance, R_{rs} , from MODIS OC, AERONET OC and the atmospheric corrections for RSP and SPEX Airborne for Case 10/23 and 10/25. The error bars for the RSP retrieved results with cost functions of $7\rho_t$ and $7\rho_t + 5P_t$ indicate one sigma retrieval uncertainties. SPEX Airborne atmospheric correction use the same RSP retrieved aerosol models and therefore shares the same retrieval uncertainties (not indicated in plot). The error bar for the AERONET OC R_{rs} indicates its daily variation.

The RSP and 410 nm band is excluded from comparison due to the observation of 4% decrease in its radiometric throughput, while other RSP bands maintain stable within $\sim 1\%$ in the radiometric calibration and $\sim 0.1\%$ in the polarimetric calibration (Knobelspiesse et al., 2020). The SPEX R_{rs} at wavelengths shorter than 470 nm are not compared due to the large because of the observed absolute systematic difference in the with the RSP 410 and 470 nm bands as discussed in Section 2. The retrieved 5 RSP R_{rs} using the aerosol properties from $7\rho_t + 5P_t$ and $7\rho_t$ shows similar values and uncertainties for both Case 10/23 and 10/25, therefore we only compare MODIS and AERONET results with 25. The following discussions refer to RSP R_{rs} from results with cost function $7\rho_t + 5P_t$. RSP R_{rs} shows good agreements with AERONET R_{rs} for both cases. As shown in Table 3, The RSP R_{rs} at 470 and 550 nm are 0.0026 and 0.0020 respectively for Case 10/25 shows good agreement between 23, and 10 0.0025 and 0.0021 respectively for Case 10/25. For AERONET R_{rs} , the values at 442, 490 and 550 nm are 0.0027, 0.0028, 0.0017 sr^{-1} for Case 10/23 and 0.0028, 0.0029, 0.0017 sr^{-1} for Case 10/25. Using the interpolated value of AERONET R_{rs} at RSP bands, the difference between RSP and AERONET R_{rs} are within 0.0003 sr^{-1} .

When comparing R_{rs} from SPEX Airborne, RSP, MODIS OC and AERONET OC. At 470 nm, the RSP and, Case 10/25 shows good agreements. SPEX R_{rs} are 0.0025 at 470 and 0.0022 sr^{-1} , and at 550 nm, they are 0.0021 are 0.0022 and 0.0017 sr^{-1} with a difference with AERONET and RSP R_{rs} less than 0.0004 sr^{-1} . For Case 10/23, the SPEX R_{rs} spectrum is consistent with the AERONET and RSP results for the wavelengths longer than 500 nm, while R_{rs} from SPEX is smaller than both AERONET and RSP at shorter wavelengths. At 470 nm, the RSP and SPEX R_{rs} are 0.0026 and is 0.0014 sr^{-1} respectively, and the MODIS R_{rs} is in between. The difference of the MODIS and SPEX of RSP and SPEX R_{rs} . The maximum difference between SPEX R_{rs} and the AERONET R_{rs} is around 0.001 sr^{-1} at 470 nm which is larger than the retrieval uncertainty of 0.0003 sr^{-1} as shown in Table 3. Note that the PACE requirement on the water-leaving reflectance between 400-600 nm is 20 0.002 or 5% (Werdell et al., 2019), which corresponds to 0.0006 sr^{-1} in R_{rs} . The R_{rs} retrieval uncertainties and difference between RSP and AERONET R_{rs} are within this requirement, but the difference between SPEX and AERONET R_{rs} for

Case 10/23 is larger than the requirement. The larger difference of RSP, SPEX and MODIS R_{rs} at wavelengths smaller than 500 nm may be related to the measurement uncertainties where the ~~effects are larger for the same percentage uncertainties due to the larger total measurement values~~, reflectance are larger at shorter wavelengths. Another possible reason for the discrepancy between the MODIS R_{rs} and others is the different aerosol models used for atmospheric correction; for MODIS, 5 it is determined from the two NIR bands of 748 and 869 nm while others are based on polarimeter retrievals.

As shown in Fig. 6, for both Case 10/23 and 10/25, there are two small dips between 600 and ~~700nm~~–700 nm in the remote sensing reflectance which are related to the oxygen absorption bands peaked at 688 nm (B-band) and 629 nm (γ band). It is challenging to correct for the impacts from the strong gas absorption due to interaction between multiple scattering and gas absorption. ~~In future studies any~~ ~~Further~~ improvement requires knowledge of aerosol height and the exact instrument line shape 10 function.

5 Discussion

Accurate determination of water leaving signals is key to derive ocean water optical properties and ocean biogeochemical conditions. In this work we have shown an example of how information rich observations of the atmosphere (from a MAP) can be used to perform an atmospheric correction ~~for on~~ highly spectrally resolved measurements of the ocean. As discussed 15 in Section 2, ~~there are systematic differences between RSP and SPEX Airborne at 410 nm and 470 nm with values reflectance measured by RSP is larger than SPEX Airborne measurement by a systematic difference of 4% and 3% respectively at 410 and 470 nm respectively~~. The impact on the aerosol retrievals are likely mitigated by relying more on the polarization information with much smaller uncertainties than reflectance and better agreement between RSP and SPEX Airborne measurements, but the computation of the water leaving signals cannot avoid the bias in reflectance. The atmospheric correction process requires 20 the subtraction of the total measured reflectance by the simulated contributions from atmosphere and ocean surface. Therefore, the uncertainties and bias in the measurements can directly impact the water leaving signals retrievals. The reflectances ρ_t measured ~~are~~ by RSP at 410 and 470 nm are 0.15 and 0.09, respectively. Based on the definition of R_{rs} , the 4% and 3% systematic difference in ~~the~~ reflectance will transfer into ~~a large~~ R_{rs} biases around 0.002 and 0.0009 ~~rs⁻¹ as large as more than half of the total water leaving signals~~. ~~sr⁻¹~~. Therefore the R_{rs} from both RSP and SPEX Airborne with wavelengths 25 less than 470 nm are not compared. The random difference between RSP and SPEX measurements at 470 nm band is 2% as discussed by Smit et al. (2019) which can transfer to 0.0006 ~~sr⁻¹~~ in R_{rs} . The differences of the R_{rs} from RSP and SPEX at 470 nm (0.0012 for Case 10/23 and 0.0003 for Case 10/25 with $7\rho_t + 5P_t$) may be due to the combined effects of the random and systematic differences in their measurements.

Accurate retrieval of R_{rs} requires a higher level of measurement accuracy, especially for the shorter wavelengths where 30 the total reflectance is more dominated by the contribution of Rayleigh scattering. To remove the bias in measurement and improve atmospheric corrections, vicarious correction techniques using ground-based measurements has been developed for ocean color radiometry (Franz et al., 2007), and have also been applied to hyperspectral measurements (Ibrahim et al., 2018). Cross calibration between a MAP and hyperspectral radiometer will be critical for combining their results together for the pur-

pose of ocean color remote sensing. Challenges in the measurement accuracy for ocean color observations will be addressed in the PACE mission, where the hyperspectral OCI measurement will achieve high calibration accuracies through pre-launch calibration campaigns, on-orbit gain adjustment through solar diffuser and lunar measurements, and on-orbit vicarious calibration (Werdell et al., 2019). On-orbit MAP cross-calibration with OCI will be possible – for example, measurements at the $\pm 20^\circ$ viewing angle of SPEXone are expected to be cross-calibrated with OCI, transferring the high radiometric accuracy from OCI to SPEXone (Werdell et al., 2019)

Aerosol micro-physical properties are important to compute their optical properties and conduct atmospheric correction. As shown in Table 3, the retrieved R_{rs} for both Cases 10/23 and 10/25 is not sensitive to the exact aerosol micro-physical properties. Both $7\rho_t$ and $7\rho_t + 5P_t$ produce similar R_{rs} and small relative uncertainties of $0.0003 \sim 0.0004 sr^{-1}$ at 470 nm. This is due to the small aerosol loading, the relatively simple aerosol micro-physical properties with almost no absorption, and the flat spectral dependency of the refractive index in ~~VIS. A complete evaluation of the impact of the aerosol properties retrieved from MAP on atmospheric correction requires studies with more complex aerosol properties such as absorbing aerosols, which will be a subject of study in the future.~~

the visible bands. Meanwhile, we have shown polarization information can help to ~~improve accuracy~~ ~~reduce retrieval uncertainties~~ in the retrieval of aerosol optical depth, fine mode refractive index and SSA as shown in Fig. 5. ~~These reduced uncertainties~~ ~~Table 3~~, but the retrieval accuracies are limited by the low AOD. Besides the theoretical retrieval accuracy analysis, validations with direct measurements are important to account for unknown uncertainties. The AOD results from polarimetric retrievals can be validated with ground-based measurement such as AERONET and lidar measurements such as HSRL, however, it is challenging to validate complex aerosol refractive index, SSA, and size distribution for the entire atmospheric column due to the lack of direct measurements. Such validation requires well-planned airborne field campaigns, concepts for which are under development (PACE Science Data Product Validation Plan). The reduced retrieval uncertainties ~~from polarimetric retrievals~~ in the aerosol micro-physical properties can ~~potentially~~ help to determine aerosol type and its composition ~~when there is sufficient aerosol loading~~, and therefore provide valuable information in the study of aerosol deposition to the ocean and its impact on the ocean ecosystem and, potentially, the role of the ocean in aerosol formation. ~~Based on the aerosol properties retrieved for Case 10/23 and 10/25 as shown in Fig. 5, we derived an aerosol type from the aerosol refractive index, SSA and extinction angstrom exponent (EAE) defined as $EAE = -\ln(AOD_{\lambda_1}/AOD_{\lambda_2})/\ln(\lambda_1/\lambda_2)$ (Russell et al., 2014), where seven aerosol types are defined: pure dust, polluted dust, urban-industrial/developed economy, urban-industrial/developing economy, biomass burning/white smoke, biomass burning/dark smoke, and pure marine. Since the fine mode and coarse mode refractive indices are independent parameters in our retrievals, we perform the aerosol typing separately for the fine and coarse modes. For the Case 10/23 retrieval after adding polarization, the fine mode refractive index at 550 nm increases from 1.47 to 1.61 with much reduced uncertainties, and the fine mode SSA increased from 0.91 to 0.99. The EAE computed using 470 and 865 nm for the fine mode AOD changes from 2.1 to 1.1. Following the typing scheme from Russell et al. (2014), with the polarization information, the fine mode particle could be interpreted as polluted dust, while with reflectance only results, the aerosol type may fall into the biomass burning type with higher EAE values and refractive index. For coarse mode aerosols, we observe large uncertainties for the volume distribution and refractive index, and therefore it is challenging to determine its~~

aerosol type accurately. The large uncertainties in coarse model aerosol properties may be due to the small contribution of the coarse mode signal in the total reflectance and the neglect of the SWIR DoLP in retrievals.

Furthermore, the retrieval uncertainties evaluated in this study are for the retrievals converged within a range of cost function value [χ^2_{min} , $\chi^2_{min} + 1$]. This approach provides a statistical evaluation of the uncertainties relating to the cost function sensitivity and impact of initial values. When considering [χ^2_{min} , $\chi^2_{min} + 3$], 50% of data considered for $7\rho_t + 5P_t$ and 80% for $7\rho_t$ fall in this range as shown in Fig 4 (b), which lead to the uncertainties of fine mode refractive index increasing to $0.04 \sim 0.05$ for $7\rho_t + 5P_t$, still smaller than the uncertainties of $7\rho_t$ with a value around $0.08 \sim 0.1$ (Fig 7). The choice of cut-off cost function value used for retrievals in practice would depend on the accuracy requirement and the algorithm to determine the initial values. The study by Knobelspiesse et al. (2012) estimated retrieval uncertainties using the error propagation method for the Aerosol Polarimetry Sensor (APS) (similar to RSP characteristics used in this study, although they used SWIR polarization) with various optical depths and aerosol types. The solar zenith and azimuth angles used by Knobelspiesse et al. (2012) are both 45° , which are similar to the solar zenith angles $\sim 50^\circ$ used in this study and in between of the two solar azimuth angles (8.7° and 94.6°) as shown in Table 1. Their results showed the uncertainties for fine mode refractive index, SSA and total AOD to be 0.015, 0.02 and 0.005 when $AOD = 0.039$. The corresponding uncertainties evaluated in this study with a similar AOD are $0.02 \sim 0.03$, $0.02 \sim 0.04$ and 0.004 for fine mode refractive index, SSA and total AOD as shown in Table 3. The uncertainties of the retrieval parameters evaluated using random initial values may not represent the full uncertainties in the retrievals. However, the two

The uncertainty results computed from two completely different approaches are comparable to each other, which may relate to the intrinsic sensitivity of the cost functions when converged close to the global minimum in the retrievals. in magnitudes. The error propagation method directly relates the retrieval uncertainties to the measurement uncertainties by projecting them from measurement to state space using Jacobians calculated from the radiative transfer model. This method accurately represents retrieval uncertainty if: (1) the measurement uncertainty is correct, (2) the forward model is an accurate and complete representation of physical reality, (3) the state space is locally linear about the retrieval, and (4) the retrieval algorithm is able to successfully converge to the smallest cost function value without artifacts. In practice, (2) is nearly always approximate, and (3) and (4) are not always the case, so the methodology used in Knobelspiesse et al. (2012) can be considered the best case retrieval uncertainty. It is, however, a convenient metric for retrieval uncertainty estimation since Jacobians are often calculated as part of the retrieval process and can be reused for this purpose. The retrieval uncertainty method used in this work (expressing the volume in state space containing cost function values calculated with many retrievals performed using randomly generated initial values) is similar in some respects, as it also relies on an accurate measurement uncertainty model (1) and forward model (2). However, it may be more accurate in some cases, since it does not make the assumption of local linearity (3) and can incorporate some potential convergence artifacts (4). Because this technique requires execution of many retrievals to have a sufficient distribution of the cost functions, it is computationally inefficient for operational use. It is, however, very relevant for a (data) limited study such as this, as it provides more realistic uncertainty estimate.

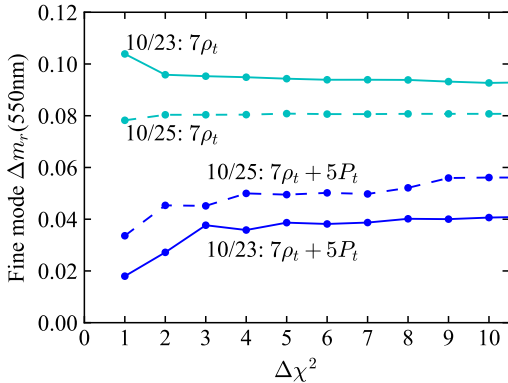


Figure 7. The uncertainties of the fine mode refractive index (Δm_r) at 550 nm computed from the cases converged within the cost function range of $[\chi^2_{min}, \chi^2_{min} + \Delta\chi^2]$ where $\Delta\chi^2$ is from 1 to 10.

6 Conclusions

We have retrieved aerosol properties using multi-angle polarimetric measurement from RSP in the ACEPOL field campaign over the AERONET USC_SEAPRISM site. The aerosol properties are then applied to the hyperspectral SPEX Airborne measurement to compute water leaving signals. This is a proof of concept for the application of MAP data on PACE to the atmospheric correction of the OCI spectrometer on the same mission. We demonstrated the improved accuracy when combining the reflectance and polarization in the retrievals compared to reflectance only retrievals. After adding DoLP in the retrieval cost functions, the uncertainties for aerosol refractive index, SSA and AOD are mostly reduced by a factor of 2 for the two cases considered in the study. The absolute values also agree better with the AERONET aerosol product except SSA probably due to the large uncertainty of SSA from both the MAP and AERONET inversions at low AOD. Moreover, the higher accuracy in DoLP measurements introduces larger weights of DoLP in the cost function relative to the reflectance measurement, and therefore provides resilience to the uncertainties and bias in the reflectance measurements, and produces a higher aerosol retrieval quality.

In order to apply the retrieved aerosol properties from the MAP measurements to hyperspectral atmospheric correction, the principal components of the aerosol refractive index spectra are interpolated into the bands specified for SPEX airborne. The retrieval parameters from MAP measurements can be used directly with the hyperspectral measurements without interpolation. The resulting hyperspectral water leaving reflectances agree well. The retrieval uncertainties on RSP R_{rs} is within 0.0004 sr^{-1} (same to SPEX R_{rs}), while the comparison of the two cases with the AERONET OC and MODIS OC products. The systematic differences between the RSP and SPEX Airborne radiometric measurements at 410 and 470 nm lead to larger discrepancies for the water leaving radiance from the SPEX airborne data. R_{rs} shows a difference less than 0.0003 sr^{-1} for RSP R_{rs} , and a maximum difference of 0.0004 sr^{-1} (Case 10/25) and 0.001 sr^{-1} (Case 10/23) for SPEX R_{rs} . The difference of SPEX R_{rs} for Case 10/23 is larger than the retrieval uncertainties, which is likely due to the radiometric uncertainties from

the sensors. In the context of the PACE mission, the aerosol properties can be retrieved from the two PACE MAPs: SPEXone and HARP2, and applied to the hyperspectral measurement from the OCI instrument which has a much higher radiometric accuracy (although SPEXone and HARP2 have different characteristics than RSP). Although the hyperspectral atmospheric correction for wavelength less than 470 nm cannot be demonstrated by the SPEX airborne data in this study, the PACE OCI
5 will provide high quality hyperspectral measurement from 340 to 890 nm and a few SWIR bands, and the demonstration of the atmospheric correction including UV spectral range will require future studies. With the MAPs and OCI on PACE, both aerosol micro-physical properties and hyperspectral ocean color signals will be obtained simultaneously with a global coverage and the knowledge will help the study, monitoring and protection of the ocean ecosystem.

Data availability. The data files for RSP, SPEX Airborne and and HSRL-2 used in this study are listed below. The RSP data is available
10 from the NASA GISS website (NASA RSP Data Site), and the SPEX L1C and HSRL-2 files are available from the ACEPOL website(<https://www-air.larc.nasa.gov/missions/acepol/index.html>).

15 – Case 10/23

RSP: RSP2-ER2_L1B-RSPGEOL1B-GeolocatedRadiances_20171023T210750Z_V001-20171024T034314Z.h5

SPEX: L1C-20171023_211047_150-213119_220_1000m_radiance.h5

15 HSRL-2: ACEPOL-HSRL2_ER2_20171023_R1.h5

– Case 10/25

RSP: RSP2-ER2_L1B-RSPGEOL1B-GeolocatedRadiances_20171025T204909Z_V001-20171026T030529Z.h5

SPEX: L1C-20171025_204857_50-210929_170_1000m_radiance.h5

HSRL-2: ACEPOL-HSRL2_ER2_20171025_R1.h5

20 *Author contributions.* MG generated the scientific data used in this paper and wrote the original manuscript. PWZ and BF formulated the original concept for this study. MG and PWZ developed the retrieval algorithm. PWZ developed the hyperspectral radiative transfer code used in this study. KK and BC advised on the retrieval uncertainty evaluation and aerosol typing. AI, BF, and YH advised on the atmospheric correction. SC advised on the aerosol interaction with the ocean. PJW advised on the PACE instruments. OH and GF provided and advised on the SPEX Airborne data. All authors participated the writing and editing of this paper.

25 *Competing interests.* The authors declare no conflict of interest.

Acknowledgements. The authors would like to thank the ACEPOL team for conducting the field campaign and providing the data, thank the Oregon State University team for maintaining the AERONET USC_SEAPRISM site. Funding for the ACEPOL campaign from the Radiation Sciences Program managed by Dr. Hal Maring is acknowledged. Part of this work is funded by the NWO/NSO project ACEPOL:

Aerosol Characterization from Polarimeter and Lidar under project number ALW-GO/16-09. M. Gao, B. Franz, B. Cairns, K. Knobelspiesse, A. Ibrahim, S. Craig, and J. Werdell acknowledge support from the NASA PACE Project. P. Zhai acknowledges support from NASA Grant 80NSSC18K0345 under the Remote Sensing of Water Quality Program. M. Gao would like to thank Ivona Cetinić, Chris Proctor and Snorre Stamnes, [Minwei Zhang](#) for constructive discussions.

References

Ahmad, Z., Franz, B. A., McClain, C. R., Kwiatkowska, E. J., Werdell, J., Shettle, E. P., and Holben, B. N.: New aerosol models for the retrieval of aerosol optical thickness and normalized water-leaving radiances from the SeaWiFS and MODIS sensors over coastal regions and open oceans, *Applied Optics*, 49, 5545–5560, 2010.

5 Anderson, G., Clough, S., Kneizys, F., Chetwynd, J., and Shettle, E.: AFGL Atmospheric Constituent Profiles (0.120km), p. 46, 1986.

Bohren, C. F. and Huffman, D. R.: *Absorption and Scattering of Light by Small Particles*, WILEY-VCH Verlag GmbH & Co. KGaA, 1998.

Burton, S. P., Hair, J. W., Kahnert, M., Ferrare, R. A., Hostetler, C. A., Cook, A. L., Harper, D. B., Berkoff, T. A., Seaman, S. T., Collins, J. E., Fenn, M. A., and Rogers, R. R.: Observations of the spectral dependence of linear particle depolarization ratio of aerosols using NASA Langley airborne High Spectral Resolution Lidar, *Atmospheric Chemistry and Physics*, 15, 13 453–13 473, <https://doi.org/10.5194/acp-15-13453-2015>, <https://www.atmos-chem-phys.net/15/13453/2015/>, 2015.

10 Cairns, B., E. Russell, E., and D. Travis, L.: Research Scanning Polarimeter: calibration and ground-based measurements, *Proc.SPIE*, 3754, 3754 – 3754 – 11, <https://doi.org/10.1117/12.366329>, <https://doi.org/10.1117/12.366329>, 1999.

Carr, M.-E., Friedrichs, M. A., Schmeltz, M., Aita, M. N., Antoine, D., Arrigo, K. R., Asanuma, I., Aumont, O., Barber, R., Behrenfeld, M., Bidigare, R., Buitenhuis, E. T., Campbell, J., Ciotti, A., Dierssen, H., Dowell, M., Dunne, J., Esaias, W., Gentili, B., Gregg, 15 Groom, S., Hoepffner, N., Ishizaka, J., Kameda, T., Quéré, C. L., Lohrenz, S., Marra, J., Mélin, F., Moore, K., Morel, A., Reddy, T. E., Ryan, J., Scardi, M., Smyth, T., Turpie, K., Tilstone, G., Waters, K., and Yamanaka, Y.: A comparison of global estimates of marine primary production from ocean color, *Deep Sea Research Part II: Topical Studies in Oceanography*, 53, 741 – 770, <https://doi.org/https://doi.org/10.1016/j.dsr2.2006.01.028>, <http://www.sciencedirect.com/science/article/pii/S0967064506000555>, the US JGOFS Synthesis and Modeling Project: Phase III, 2006.

20 Chowdhary, J., Cairns, B., Mishchenko, M., and Travis, L.: Retrieval of aerosol properties over the ocean using multispectral and multiangle Photopolarimetric measurements from the Research Scanning Polarimeter, *Geophysical Research Letters*, 28, 243–246, <https://doi.org/10.1029/2000GL011783>, <https://agupubs.onlinelibrary.wiley.com/doi/abs/10.1029/2000GL011783>, 2001.

Chowdhary, J., Cairns, B., Mishchenko, M. I., Hobbs, P. V., Cota, G. F., Redemann, J., Rutledge, K., Holben, B. N., and Russell, E.: Retrieval of Aerosol Scattering and Absorption Properties from Photopolarimetric Observations over the Ocean during the CLAMS Experiment, 25 *Journal of the Atmospheric Sciences*, 62, 1093–1117, <https://doi.org/10.1175/JAS3389.1>, <https://doi.org/10.1175/JAS3389.1>, 2005.

Chowdhary, J., Cairns, B., Waquet, F., Knobelispiesse, K., Ottaviani, M., Redemann, J., Travis, L., and Mishchenko, M.: Sensitivity of multiangle, multispectral polarimetric remote sensing over open oceans to water-leaving radiance: Analyses of RSP data acquired during the MILAGRO campaign, *Remote Sensing of Environment*, 118, 284–308, 2012.

Chowdhary, J., Stamnes, S., Zhang, M., Scarino, A., Wasilewski, A., and Cairns, B.: Combining multispectral VIS-SWIR polarimetry and 30 UV-NIR hyperspectral imagery to retrieve aerosol and ocean color properties from remote sensing: case studies for airborne RSP and GCAS observations, *American Geophysical Union, Fall Meeting*, abstract OS11D-1435, 2018.

Chowdhary, J., Zhai, P.-W., Boss, E., Dierssen, H., Frouin, R., Ibrahim, A., Lee, Z., Remer, L. A., Twardowski, M., Xu, F., Zhang, X., Ottaviani, M., Espinosa, W. R., and Ramon, D.: Modeling Atmosphere-Ocean Radiative Transfer: A PACE Mission Perspective, *Frontiers in Earth Science*, 7, 100, <https://doi.org/10.3389/feart.2019.00100>, <https://www.frontiersin.org/article/10.3389/feart.2019.00100>, 2019.

35 Cox, C. and Munk, W.: Measurement of the Roughness of the Sea Surface from Photographs of the Sun's Glitter, *J. Opt. Soc. Am.*, 44, 838–850, 1954.

Craig, S. E., Jones, C. T., Li, W. K., Lazin, G., Horne, E., Caverhill, C., and Cullen, J. J.: Deriving optical metrics of coastal phytoplankton biomass from ocean colour, *Remote Sensing of Environment*, 119, 72 – 83, <https://doi.org/10.1016/j.rse.2011.12.007>, <http://www.sciencedirect.com/science/article/pii/S0034425711004445>, 2012.

Croft, B., Martin, R. V., Leitch, W. R., Burkart, J., Chang, R. Y-W., Collins, D. B., Hayes, P. L., Hodshire, A. L., Huang, L., Kondros, J. K., Moravek, A., Mungall, E. L., Murphy, J. G., Sharma, S., Tremblay, S., Wentworth, G. R., Willis, M. D., Abbatt, J. P. D., and Pierce, J. R.: Arctic marine secondary organic aerosol contributes significantly to summertime particle size distributions in the Canadian Arctic Archipelago, *Atmospheric Chemistry and Physics*, 19, 2787–2812, <https://doi.org/10.5194/acp-19-2787-2019>, <https://www.atmos-chem-phys.net/19/2787/2019/>, 2019.

d'Almeida, G. A., Koepke, P., and Shettle, E. P.: *Atmospheric aerosols : global climatology and radiative characteristics*, A Deepak Pub, 1991.

10 Description of Aerosol Inversion Uncertainty for Level 2 Products: https://aeronet.gsfc.nasa.gov/new_web/optical_properties.html.

Dierssen, H. M. and Randolph, K.: *Remote Sensing of Ocean Color*, pp. 439–472, Springer New York, New York, NY, https://doi.org/10.1007/978-1-4614-5684-1_18, https://doi.org/10.1007/978-1-4614-5684-1_18, 2013.

Diner, D. J., Xu, F., Garay, M. J., Martonchik, J. V., Rheingans, B. E., Geier, S., Davis, A., Hancock, B. R., Jovanovic, V. M., Bull, M. A., 15 Capraro, K., Chipman, R. A., and McClain, S. C.: The Airborne Multiangle SpectroPolarimetric Imager (AirMSPI): a new tool for aerosol and cloud remote sensing, *Atmospheric Measurement Techniques*, 6, 2007–2025, <https://doi.org/10.5194/amt-6-2007-2013>, <https://www.atmos-meas-tech.net/6/2007/2013/>, 2013.

Diner, D. J., Boland, S. W., Brauer, M., Bruegge, C., Burke, K. A., Chipman, R., Girolamo, L. D., Garay, M. J., Hasheminassab, S., Hyer, E., Jerrett, M., Jovanovic, V., Kalashnikova, O. V., Liu, Y., Lyapustin, A. I., Martin, R. V., Nastan, A., Ostro, B. D., Ritz, B., Schwartz, 20 J., Wang, J., and Xu, F.: Advances in multiangle satellite remote sensing of speciated airborne particulate matter and association with adverse health effects: from MISR to MAIA, *Journal of Applied Remote Sensing*, 12, 1 – 22, <https://doi.org/10.1117/1.JRS.12.042603>, <https://doi.org/10.1117/1.JRS.12.042603>, 2018.

Dubovik, O. and King, M. D.: A flexible inversion algorithm for retrieval of aerosol optical properties from Sun and sky radiance measurements, *Journal of Geophysical Research: Atmospheres*, 105, 20 673–20 696, 2000.

25 Dubovik, O., Smirnov, A., Holben, B. N., King, M. D., Kaufman, Y. J., Eck, T. F., and Slutsker, I.: Accuracy assessments of aerosol optical properties retrieved from Aerosol Robotic Network (AERONET) Sun and sky radiance measurements, *Journal of Geophysical Research: Atmospheres*, 105, 9791–9806, <https://doi.org/10.1029/2000JD900040>, <https://agupubs.onlinelibrary.wiley.com/doi/abs/10.1029/2000JD900040>, 2000.

Dubovik, O., Sinyuk, A., Lapyonok, T., Holben, B. N., Mishchenko, M., Yang, P., Eck, T. F., Volten, H., Muñoz, O., Veihelmann, B., van der 30 Zande, W. J., Leon, J.-F., Sorokin, M., and Slutsker, I.: Application of spheroid models to account for aerosol particle nonsphericity in remote sensing of desert dust, *Journal of Geophysical Research: Atmospheres*, 111, <https://doi.org/10.1029/2005JD006619>, <https://agupubs.onlinelibrary.wiley.com/doi/abs/10.1029/2005JD006619>, 2006.

Dubovik, O., Herman, M., Holdak, A., Lapyonok, T., Tanré, D., Deuzé, J. L., Ducos, F., Sinyuk, A., and Lopatin, A.: Statistically optimized inversion algorithm for enhanced retrieval of aerosol properties from spectral multi-angle polarimetric satellite observations, *Atmospheric 35 Measurement Techniques*, 4, 975–1018, <https://doi.org/10.5194/amt-4-975-2011>, <https://www.atmos-meas-tech.net/4/975/2011/>, 2011.

Dubovik, O., Lapyonok, T., Litvinov, P., Herman, M., Fuertes, D., Ducos, F., Lopatin, A., Chaikovsky, A., Torres, B., Derimian, Y., Huang, X., Aspetsberger, M., and Federspiel, C.: GRASP: a versatile algorithm for characterizing the atmosphere, *SPIE Newsroom*, <https://doi.org/10.1117/2.1201408.005558>, 2014.

Dubovik, O., Li, Z., Mishchenko, M. I., Tanré, D., Karol, Y., Bojkov, B., Cairns, B., Diner, D. J., Espinosa, W. R., Goloub, P., Gu, X., Hasekamp, O., Hong, J., Hou, W., Knobelspiesse, K. D., Landgraf, J., Li, L., Litvinov, P., Liu, Y., Lopatin, A., Marbach, T., Maring, H., Martins, V., Meijer, Y., Milinevsky, G., Mukai, S., Parol, F., Qiao, Y., Remer, L., Rietjens, J., Sano, I., Stammes, P., Stammes, S., Sun, X., Tabary, P., Travis, L. D., Waquet, F., Xu, F., Yan, C., and Yin, D.: Polarimetric remote sensing of atmospheric aerosols: 5 Instruments, methodologies, results, and perspectives, *Journal of Quantitative Spectroscopy and Radiative Transfer*, 224, 474 – 511, <https://doi.org/https://doi.org/10.1016/j.jqsrt.2018.11.024>, <http://www.sciencedirect.com/science/article/pii/S0022407318308409>, 2019.

Eck, T. F., Holben, B. N., Reid, J. S., Dubovik, O., Smirnov, A., O'Neill, N. T., Slutsker, I., and Kinne, S.: Wavelength dependence of the optical depth of biomass burning, urban, and desert dust aerosols, *Journal of Geophysical Research: Atmospheres*, 104, 31 333–31 349, <https://doi.org/10.1029/1999JD900923>, <https://agupubs.onlinelibrary.wiley.com/doi/abs/10.1029/1999JD900923>, 1999.

10 Fan, C., Fu, G., Di Noia, A., Smit, M., H.H. Rietjens, J., A. Ferrare, R., Burton, S., Li, Z., and P. Hasekamp, O.: Use of A Neural Network-Based Ocean Body Radiative Transfer Model for Aerosol Retrievals from Multi-Angle Polarimetric Measurements, *Remote Sensing*, 11, <https://doi.org/10.3390/rs11232877>, <https://www.mdpi.com/2072-4292/11/23/2877>, 2019.

Fedarenka, A., Dubovik, O., Goloub, P., Li, Z., Lapyonok, T., Litvinov, P., Barel, L., Gonzalez, L., Podvin, T., and Crozel, D.: Utilization of 15 AERONET polarimetric measurements for improving retrieval of aerosol microphysics: GSFC, Beijing and Dakar data analysis, *Journal of Quantitative Spectroscopy and Radiative Transfer*, 179, 72 – 97, <https://doi.org/https://doi.org/10.1016/j.jqsrt.2016.03.021>, <http://www.sciencedirect.com/science/article/pii/S0022407316301534>, 2016.

Fichot, C. G. and Benner, R.: A novel method to estimate DOC concentrations from CDOM absorption coefficients in coastal waters, *Geophysical Research Letters*, 38, <https://doi.org/10.1029/2010GL046152>, <https://agupubs.onlinelibrary.wiley.com/doi/abs/10.1029/2010GL046152>, 2011.

20 Fougnie, B., Marbach, T., Lacan, A., Lang, R., Schlüssel, P., Poli, G., Munro, R., and Couto, A. B.: The multi-viewing multi-channel multi-polarisation imager – Overview of the 3MI polarimetric mission for aerosol and cloud characterization, *Journal of Quantitative Spectroscopy and Radiative Transfer*, 219, 23 – 32, <https://doi.org/https://doi.org/10.1016/j.jqsrt.2018.07.008>, <http://www.sciencedirect.com/science/article/pii/S002240731830373X>, 2018.

Franz, B. A., Bailey, S. W., Werdell, P. J., and McClain, C. R.: Sensor-independent approach to the vicarious calibration of satellite ocean 25 color radiometry, *Appl. Opt.*, 46, 5068–5082, <https://doi.org/10.1364/AO.46.005068>, <http://ao.osa.org/abstract.cfm?URI=ao-46-22-5068>, 2007.

Frouin, R. J., Franz, B. A., Ibrahim, A., Knobelspiesse, K., Ahmad, Z., Cairns, B., Chowdhary, J., Dierssen, H. M., Tan, J., Dubovik, O., Huang, X., Davis, A. B., Kalashnikova, O., Thompson, D. R., Remer, L. A., Boss, E., Coddington, O., Deschamps, P.-Y., Gao, B.-C., Gross, L., Hasekamp, O., Omar, A., Pelletier, B., Ramon, D., Steinmetz, F., and Zhai, P.-W.: Atmospheric Correction of Satellite Ocean-30 Color Imagery During the PACE Era, *Frontiers in Earth Science*, 7, 145, <https://doi.org/10.3389/feart.2019.00145>, <https://www.frontiersin.org/article/10.3389/feart.2019.00145>, 2019.

Fu, G. and Hasekamp, O.: Retrieval of aerosol microphysical and optical properties over land using a multimode approach, *Atmospheric Measurement Techniques*, 11, 6627–6650, <https://doi.org/10.5194/amt-11-6627-2018>, <https://www.atmos-meas-tech.net/11/6627/2018/>, 2018.

35 Fu, G., Hasekamp, O., Rietjens, J., Smit, M., Di Noia, A., Cairns, B., Wasilewski, A., Diner, D., Xu, F., Knobelspiesse, K., Gao, M., da Silva, A., Burton, S., Hostetler, C., Hair, J., and Ferrare, R.: Aerosol retrievals from the ACEPOL Campaign, *Atmospheric Measurement Techniques Discussions*, 2019, 1–30, <https://doi.org/10.5194/amt-2019-287>, <https://www.atmos-meas-tech-discuss.net/amt-2019-287/>, 2019.

Gao, M., Zhai, P.-W., Franz, B., Hu, Y., Knobelispiesse, K., Werdell, P. J., Ibrahim, A., Xu, F., and Cairns, B.: Retrieval of aerosol properties and water-leaving reflectance from multi-angular polarimetric measurements over coastal waters, *Opt. Express*, 26, 8968–8989, <https://doi.org/10.1364/OE.26.008968>, <http://www.opticsexpress.org/abstract.cfm?URI=oe-26-7-8968>, 2018.

Gao, M., Zhai, P.-W., Franz, B. A., Hu, Y., Knobelispiesse, K., Werdell, P. J., Ibrahim, A., Cairns, B., and Chase, A.: Inversion of multiangular polarimetric measurements over open and coastal ocean waters: a joint retrieval algorithm for aerosol and water-leaving radiance properties, *Atmospheric Measurement Techniques*, 12, 3921–3941, <https://doi.org/10.5194/amt-12-3921-2019>, <https://www.atmos-meas-tech.net/12/3921/2019/>, 2019.

Gelaro, R., McCarty, W., Suárez, M. J., Todling, R., Molod, A., Takacs, L., Randles, C. A., Darmenov, A., Bosilovich, M. G., Reichle, R., Wargan, K., Coy, L., Cullather, R., Draper, C., Akella, S., Buchard, V., Conaty, A., da Silva, A. M., Gu, W., Kim, G.-K., Koster, R., Lucchesi, R., Merkova, D., Nielsen, J. E., Partyka, G., Pawson, S., Putman, W., Rienecker, M., Schubert, S. D., Sienkiewicz, M., and Zhao, B.: The Modern-Era Retrospective Analysis for Research and Applications, Version 2 (MERRA-2), *Journal of Climate*, 30, 5419–5454, <https://doi.org/10.1175/JCLI-D-16-0758.1>, <https://doi.org/10.1175/JCLI-D-16-0758.1>, 2017.

Giles, D. M., Sinyuk, A., Sorokin, M. G., Schafer, J. S., Smirnov, A., Slutsker, I., Eck, T. F., Holben, B. N., Lewis, J. R., Campbell, J. R., Welton, E. J., Korkin, S. V., and Lyapustin, A. I.: Advancements in the Aerosol Robotic Network (AERONET) Version 3 database – automated near-real-time quality control algorithm with improved cloud screening for Sun photometer aerosol optical depth (AOD) measurements, *Atmospheric Measurement Techniques*, 12, 169–209, <https://doi.org/10.5194/amt-12-169-2019>, <https://www.atmos-meas-tech.net/12/169/2019/>, 2019.

Gordon, H. R. and Wang, M.: Retrieval of water-leaving radiance and aerosol optical thickness over the oceans with SeaWiFS: a preliminary algorithm, *Applied Optics*, 33, 443–452, 1994.

Hair, J. W., Hostetler, C. A., Cook, A. L., Harper, D. B., Ferrare, R. A., Mack, T. L., Welch, W., Izquierdo, L. R., and Hovis, F. E.: Airborne High Spectral Resolution Lidar for profiling aerosol optical properties, *Applied Optics*, 47, 6734–6752, <https://doi.org/10.1364/AO.47.006734>, <http://ao.osa.org/abstract.cfm?URI=ao-47-36-6734>, 2008.

Hasekamp, O. P. and Landgraf, J.: Retrieval of aerosol properties over land surfaces: capabilities of multiple-viewing-angle intensity and polarization measurements, *Appl. Opt.*, 46, 3332–3344, <https://doi.org/10.1364/AO.46.003332>, <http://ao.osa.org/abstract.cfm?URI=ao-46-16-3332>, 2007.

Hasekamp, O. P., Litvinov, P., and Butz, A.: Aerosol properties over the ocean from PARASOL multiangle photopolarimetric measurements, *Journal of Geophysical Research: Oceans*, 116, D14 204, 2011.

Hasekamp, O. P., Fu, G., Rusli, S. P., Wu, L., Noia, A. D., aan de Brugh, J., Landgraf, J., Smit, J. M., Rietjens, J., and van Amerongen, A.: Aerosol measurements by SPEXone on the NASA PACE mission: expected retrieval capabilities, *Journal of Quantitative Spectroscopy and Radiative Transfer*, 227, 170 – 184, <https://doi.org/https://doi.org/10.1016/j.jqsrt.2019.02.006>, <http://www.sciencedirect.com/science/article/pii/S0022407318308653>, 2019.

Holben, B., Eck, T., Slutsker, I., Tanré, D., Buis, J., Setzer, A., Vermote, E., Reagan, J., Kaufman, Y., Nakajima, T., Lavenu, F., Jankowiak, I., and Smirnov, A.: AERONET—A Federated Instrument Network and Data Archive for Aerosol Characterization, *Remote Sensing of Environment*, 66, 1 – 16, [https://doi.org/https://doi.org/10.1016/S0034-4257\(98\)00031-5](https://doi.org/https://doi.org/10.1016/S0034-4257(98)00031-5), <http://www.sciencedirect.com/science/article/pii/S0034425798000315>, 1998.

Holben, B. N., Tanré, D., Smirnov, A., Eck, T. F., Slutsker, I., Abu Hassan, N., Newcomb, W. W., Schafer, J. S., Chatenet, B., Lavenu, F., Kaufman, Y. J., Castle, J. V., Setzer, A., Markham, B., Clark, D., Frouin, R., Halthore, R., Karneli, A., O'Neill, N. T., Pietras, C., Pinker, R. T., Voss, K., and Zibordi, G.: An emerging ground-based aerosol climatology: Aerosol optical depth from AERONET, *Journal*

of Geophysical Research: Atmospheres, 106, 12 067–12 097, <https://doi.org/10.1029/2001JD900014>, <https://agupubs.onlinelibrary.wiley.com/doi/abs/10.1029/2001JD900014>, 2001.

5 Hu, C., Feng, L., and Lee, Z.: Uncertainties of SeaWiFS and MODIS remote sensing reflectance: Implications from clear water measurements, *Remote Sensing of Environment*, 133, 168 – 182, <https://doi.org/https://doi.org/10.1016/j.rse.2013.02.012>, <http://www.sciencedirect.com/science/article/pii/S0034425713000539>, 2013.

Ibrahim, A., Franz, B., Ahmad, Z., Healy, R., Knobelispiesse, K., Gao, B.-C., Proctor, C., and Zhai, P.-W.: Atmospheric correction for hyperspectral ocean color retrieval with application to the Hyperspectral Imager for the Coastal Ocean (HICO), *Remote Sensing of Environment*, 204, 60 – 75, <https://doi.org/https://doi.org/10.1016/j.rse.2017.10.041>, <http://www.sciencedirect.com/science/article/pii/S0034425717305047>, 2018.

10 Ibrahim, A., Franz, B. A., Ahmad, Z., and Bailey, S. W.: Multiband Atmospheric Correction Algorithm for Ocean Color Retrievals, *Frontiers in Earth Science*, 7, 116, <https://doi.org/10.3389/feart.2019.00116>, <https://www.frontiersin.org/article/10.3389/feart.2019.00116>, 2019.

Jamet, C., Ibrahim, A., Ahmad, Z., Angelini, F., Babin, M., Behrenfeld, M. J., Boss, E., Cairns, B., Churnside, J., Chowdhary, J., Davis, A. B., Dionisi, D., Duforêt-Gaurier, L., Franz, B., Frouin, R., Gao, M., Gray, D., Hasekamp, O., He, X., Hostetler, C., Kalashnikova, O. V., Knobelispiesse, K., Lacour, L., Loisel, H., Martins, V., Rehm, E., Remer, L., Sanhaj, I., Stamnes, K., Stamnes, S., Victori, S., 15 Werdell, J., and Zhai, P.-W.: Going Beyond Standard Ocean Color Observations: Lidar and Polarimetry, *Frontiers in Marine Science*, 6, 251, <https://doi.org/10.3389/fmars.2019.00251>, <https://www.frontiersin.org/article/10.3389/fmars.2019.00251>, 2019.

Kaufman, Y. J., Martins, J. V., Remer, L. A., Schoeberl, M. R., and Yamasoe, M. A.: Satellite retrieval of aerosol absorption over the oceans using sunglint, *Geophysical Research Letters*, 29, 34–1–34–4, <https://doi.org/10.1029/2002GL015403>, <https://agupubs.onlinelibrary.wiley.com/doi/abs/10.1029/2002GL015403>, 2002.

20 Kawata, Y.: Circular polarization of sunlight reflected by planetary atmospheres, *Icarus*, 33, 217 – 232, [https://doi.org/https://doi.org/10.1016/0019-1035\(78\)90035-0](https://doi.org/https://doi.org/10.1016/0019-1035(78)90035-0), <http://www.sciencedirect.com/science/article/pii/0019103578900350>, 1978.

Knobelispiesse, K., Cairns, B., Mishchenko, M., Chowdhary, J., Tsigaris, K., van Diedenhoven, B., Martin, W., Ottaviani, M., and Alexandrov, M.: Analysis of fine-mode aerosol retrieval capabilities by different passive remote sensing instrument designs, *Optics Express*, 20, 25 21 457–21 484, <https://doi.org/10.1364/OE.20.021457>, <http://www.opticsexpress.org/abstract.cfm?URI=oe-20-19-21457>, 2012.

Knobelispiesse, K., Tan, Q., Bruegge, C., Cairns, B., Chowdhary, J., van Diedenhoven, B., Diner, D., Ferrare, R., van Harten, G., Jovanovic, V., Ottaviani, M., Redemann, J., Seidel, F., and Sinclair, K.: Intercomparison of airborne multi-angle polarimeter observations from the Polarimeter Definition Experiment, *Appl. Opt.*, 58, 650–669, <https://doi.org/10.1364/AO.58.000650>, <http://ao.osa.org/abstract.cfm?URI=ao-58-3-650>, 2019.

30 Knobelispiesse, K., Barbosa, H. M. J., Bradley, C., Bruegge, C., Cairns, B., Chen, G., Chowdhary, J., Cook, A., Di Noia, A., van Diedenhoven, B., Diner, D. J., Ferrare, R., Fu, G., Gao, M., Garay, M., Hair, J., Harper, D., van Harten, G., Hasekamp, O., Helmlinger, M., Hostetler, C., Kalashnikova, O., Kupchock, A., Longo De Freitas, K., Maring, H., Martins, J. V., McBride, B., McGill, M., Norlin, K., Puthukkudy, A., Rheingans, B., Rietjens, J., Seidel, F. C., da Silva, A., Smit, M., Stamnes, S., Tan, Q., Val, S., Wasilewski, A., Xu, F., Xu, X., and Yorks, J.: The Aerosol Characterization from Polarimeter and Lidar (ACEPOL) airborne field campaign, *Earth System Science Data Discussions*, 35 2020, 1–38, <https://doi.org/10.5194/essd-2020-76>, <https://www.earth-syst-sci-data-discuss.net/essd-2020-76/>, 2020.

Li, Z., Hou, W., Hong, J., Zheng, F., Luo, D., Wang, J., Gu, X., and Qiao, Y.: Directional Polarimetric Camera (DPC): Monitoring aerosol spectral optical properties over land from satellite observation, *Journal of Quantitative Spectroscopy and Radiative Transfer*, 218, 21 – 37, <https://doi.org/https://doi.org/10.1016/j.jqsrt.2018.07.003>, <http://www.sciencedirect.com/science/article/pii/S002240731830253X>, 2018.

Mahowald, N. M., Baker, A. R., Bergametti, G., Brooks, N., Duce, R. A., Jickells, T. D., Kubilay, N., Prospero, J. M., and Tegen, I.: Atmospheric global dust cycle and iron inputs to the ocean, *Global Biogeochemical Cycles*, 19, <https://doi.org/10.1029/2004GB002402>, <https://agupubs.onlinelibrary.wiley.com/doi/abs/10.1029/2004GB002402>, 2005.

Martins, J. V., Fernandez-Borda, R., McBride, B., Remer, L., and Barbosa, H. M. J.: The Harp Hype Ran Gular Imaging Polarimeter and the Need for Small Satellite Payloads with High Science Payoff for Earth Science Remote Sensing, in: *IGARSS 2018 - 2018 IEEE International Geoscience and Remote Sensing Symposium*, pp. 6304–6307, <https://doi.org/10.1109/IGARSS.2018.8518823>, 2018.

McBride, B. A., Martins, J. V., Barbosa, H. M. J., Birmingham, W., and Remer, L. A.: Spatial distribution of cloud droplet size properties from Airborne Hyper-Angular Rainbow Polarimeter (AirHARP) measurements, *Atmospheric Measurement Techniques Discussions*, 2019, 1–32, <https://doi.org/10.5194/amt-2019-380>, <https://www.atmos-meas-tech-discuss.net/amt-2019-380/>, 2019.

McCoy, D. T., Burrows, S. M., Wood, R., Grosvenor, D. P., Elliott, S. M., Ma, P.-L., Rasch, P. J., and Hartmann, D. L.: Natural aerosols explain seasonal and spatial patterns of Southern Ocean cloud albedo, *Science Advances*, 1, <https://doi.org/10.1126/sciadv.1500157>, <https://advances.sciencemag.org/content/1/6/e1500157>, 2015.

McGill, M., Hlavka, D., Hart, W., Scott, V. S., Spinhirne, J., and Schmid, B.: Cloud Physics Lidar: instrument description and initial measurement results, *Appl. Opt.*, 41, 3725–3734, <https://doi.org/10.1364/AO.41.003725>, <http://ao.osa.org/abstract.cfm?URI=ao-41-18-3725>, 2002.

Mishchenko, M. I. and Travis, L. D.: Satellite retrieval of aerosol properties over the ocean using polarization as well as intensity of reflected sunlight, *Journal of Geophysical Research: Atmospheres*, 102, 16989–17013, <https://doi.org/10.1029/96JD02425>, <https://agupubs.onlinelibrary.wiley.com/doi/abs/10.1029/96JD02425>, 1997.

Mobley, C. D., Werdell, J., Franz, B., Ahmad, Z., and Bailey, S.: Atmospheric Correction for Satellite Ocean Color Radiometry, *National Aeronautics and Space Administration*, 2016.

NASA Ocean Color Web: <https://oceancolor.gsfc.nasa.gov/atbd/rrs/>.

NASA RSP Data Site: <https://data.giss.nasa.gov/pub/rsp>.

O'Dowd, C. D., Jimenez, J. L., Bahreini, R., Flagan, R. C., Seinfeld, J. H., Hämeri, K., Pirjola, L., Kulmala, M., Jennings, S. G., and Hoffmann, T.: Marine aerosol formation from biogenic iodine emissions, *Nature*, 417, 632–636, <https://doi.org/10.1038/nature00775>, 2002.

Ottaviani, M., Knobelispiesse, K., Cairns, B., and Mishchenko, M.: Information content of aerosol retrievals in the sunglint region, *Geophysical Research Letters*, 40, 631–634, <https://doi.org/10.1002/grl.50148>, <https://agupubs.onlinelibrary.wiley.com/doi/abs/10.1002/grl.50148>, 2013.

PACE: Pre-Aerosol,Clouds, and ocean Ecosystem (PACE) Mission Science Definition Team Report, *The National Aeronautics and Space Administration (NASA)*, https://pace.oceansciences.org/docs/PACE_TM2018-219027_Vol_2.pdf, 2018.

PACE Science Data Product Validation Plan: https://pace.oceansciences.org/docs/PACE_Validation_Plan_DRAFT_version_24March2020_posted.pdf.

Remer, L. A., Davis, A. B., Mattoo, S., Levy, R. C., Kalashnikova, O. V., Coddington, O., Chowdhary, J., Knobelispiesse, K., Xu, X., Ahmad, Z., Boss, E., Cairns, B., Dierssen, H. M., Diner, D. J., Franz, B., Frouin, R., Gao, B.-C., Ibrahim, A., Martins, J. V., Omar, A. H., Torres, O., Xu, F., and Zhai, P.-W.: Retrieving Aerosol Characteristics From the PACE Mission, Part 1: Ocean Color Instrument, *Frontiers in Earth Science*, 7, 152, <https://doi.org/10.3389/feart.2019.00152>, <https://www.frontiersin.org/article/10.3389/feart.2019.00152>, 2019a.

Remer, L. A., Knobelispiesse, K., Zhai, P.-W., Xu, F., Kalashnikova, O. V., Chowdhary, J., Hasekamp, O., Dubovik, O., Wu, L., Ahmad, Z., Boss, E., Cairns, B., Coddington, O., Davis, A. B., Dierssen, H. M., Diner, D. J., Franz, B., Frouin, R., Gao, B.-C., Ibrahim, A., Levy,

R. C., Martins, J. V., Omar, A. H., and Torres, O.: Retrieving Aerosol Characteristics From the PACE Mission, Part 2: Multi-Angle and Polarimetry, *Frontiers in Environmental Science*, 7, 94, <https://doi.org/10.3389/fenvs.2019.00094>, <https://www.frontiersin.org/article/10.3389/fenvs.2019.00094>, 2019b.

Rietjens, J., Campo, J., Chanumolu, A., Smit, M., Nalla, R., Fernandez, C., Dingjan, J., van Amerongen, A., and Hasekamp, O.: Expected 5 performance and error analysis for SPEXone, a multi-angle channeled spectropolarimeter for the NASA PACE mission, in: *Polarization Science and Remote Sensing IX*, edited by Craven, J. M., Shaw, J. A., and Snik, F., vol. 11132, pp. 34 – 47, International Society for Optics and Photonics, SPIE, <https://doi.org/10.1117/12.2530729>, <https://doi.org/10.1117/12.2530729>, 2019.

Russell, P. B., Kacenelenbogen, M., Livingston, J. M., Hasekamp, O. P., Burton, S. P., Schuster, G. L., Johnson, M. S., Knobelispiesse, K. D., Redemann, J., Ramachandran, S., and Holben, B.: A multiparameter aerosol classification method and its application to retrievals 10 from spaceborne polarimetry, *Journal of Geophysical Research: Atmospheres*, 119, 9838–9863, <https://doi.org/10.1002/2013JD021411>, <https://agupubs.onlinelibrary.wiley.com/doi/abs/10.1002/2013JD021411>, 2014.

Shettle, E. P. and Fenn, R. W.: Models for the aerosols of the lower atmosphere and the effects of humidity variations on their optical properties, *Environmental Research Papers*, Air Force Geophysics Lab., Hanscom AFB, MA. Optical Physics Div, 1979.

Siegel, D. A., Buesseler, K. O., Doney, S. C., Sailley, S. F., Behrenfeld, M. J., and Boyd, P. W.: Global assessment of 15 ocean carbon export by combining satellite observations and food-web models, *Global Biogeochemical Cycles*, 28, 181–196, <https://doi.org/10.1002/2013GB004743>, <https://agupubs.onlinelibrary.wiley.com/doi/abs/10.1002/2013GB004743>, 2014.

Smirnov, A., Holben, B., Eck, T., Dubovik, O., and Slutsker, I.: Cloud-Screening and Quality Control Algorithms for the AERONET Database, *Remote Sensing of Environment*, 73, 337 – 349, [https://doi.org/https://doi.org/10.1016/S0034-4257\(00\)00109-7](https://doi.org/https://doi.org/10.1016/S0034-4257(00)00109-7), <http://www.sciencedirect.com/science/article/pii/S0034425700001097>, 2000.

Smit, J. M., Rietjens, J. H. H., van Harten, G., Noia, A. D., Laauwen, W., Rheingans, B. E., Diner, D. J., Cairns, B., Wasilewski, A., 20 Knobelispiesse, K. D., Ferrare, R., and Hasekamp, O. P.: SPEX airborne spectropolarimeter calibration and performance, *Appl. Opt.*, 58, 5695–5719, <https://doi.org/10.1364/AO.58.005695>, <http://ao.osa.org/abstract.cfm?URI=ao-58-21-5695>, 2019.

Stamnes, S., Hostetler, C., Ferrare, R., Burton, S., Liu, X., Hair, J., Hu, Y., Wasilewski, A., Martin, W., van Diedenhoven, B., Chowdhary, J., Cetinić, I., Berg, L. K., Stamnes, K., and Cairns, B.: Simultaneous polarimeter retrievals of microphysical aerosol and ocean color 25 parameters from the “MAPP” algorithm with comparison to high-spectral-resolution lidar aerosol and ocean products, *Appl. Opt.*, 57, 2394–2413, <https://doi.org/10.1364/AO.57.002394>, <http://ao.osa.org/abstract.cfm?URI=ao-57-10-2394>, 2018.

Tanré, D., Bréon, F. M., Deuzé, J. L., Dubovik, O., Ducos, F., François, P., Goloub, P., Herman, M., Lifermann, A., and Waquet, F.: Remote sensing of aerosols by using polarized, directional and spectral measurements within the A-Train: the PARASOL mission, *Atmos. Meas. Tech.*, 4, 1383–1395, <https://doi.org/https://doi.org/10.5194/amt-4-1383-2011>, 2011.

Wang, J., Xu, X., Ding, S., Zeng, J., Spurr, R., Liu, X., Chance, K., and Mishchenko, M.: A numerical testbed for remote sensing of 30 aerosols, and its demonstration for evaluating retrieval synergy from a geostationary satellite constellation of GEO-CAPE and GOES-R, *Journal of Quantitative Spectroscopy and Radiative Transfer*, 146, 510 – 528, <https://doi.org/https://doi.org/10.1016/j.jqsrt.2014.03.020>, <http://www.sciencedirect.com/science/article/pii/S0022407314001368>, *electromagnetic and Light Scattering by Nonspherical Particles XIV*, 2014.

Wang, M., ed.: *Atmospheric Correction for Remotely-Sensed Ocean-Colour*, International Ocean Colour Coordinating Group (IOCCG), 35 2010.

Werdell, P. J., Behrenfeld, M. J., Bontempi, P. S., Boss, E., Cairns, B., Davis, G. T., Franz, B. A., Gliese, U. B., Gorman, E. T., Hasekamp, O., Knobelispiesse, K. D., Mannino, A., Martins, J. V., McClain, C. R., Meister, G., and Remer, L. A.: The Plankton,

Aerosol, Cloud, Ocean Ecosystem Mission: Status, Science, Advances, *Bulletin of the American Meteorological Society*, 100, 1775–1794, <https://doi.org/10.1175/BAMS-D-18-0056.1>, <https://doi.org/10.1175/BAMS-D-18-0056.1>, 2019.

Westberry, T., Shi, Y., Yu, H., Behrenfeld, M., and Remer, L.: Satellite-Detected Ocean Ecosystem Response to Volcanic Eruptions in the Subarctic Northeast Pacific Ocean, *Geophysical Research Letters*, 46, 11 270–11 280, <https://doi.org/10.1029/2019GL083977>, <https://agupubs.onlinelibrary.wiley.com/doi/abs/10.1029/2019GL083977>, 2019.

5 Wu, L., Hasekamp, O., van Diedenhoven, B., and Cairns, B.: Aerosol retrieval from multiangle, multispectral photopolarimetric measurements: importance of spectral range and angular resolution, *Atmospheric Measurement Techniques*, 8, 2625–2638, <https://doi.org/10.5194/amt-8-2625-2015>, <https://www.atmos-meas-tech.net/8/2625/2015/>, 2015.

Xu, F., Dubovik, O., Zhai, P. W., Diner, D. J., Kalashnikova, O. V., Seidel, F. C., Litvinov, P., Bovchaliuk, A., Garay, M. J., van Harten, G.,
10 and Davis, A. B.: Joint retrieval of aerosol and water-leaving radiance from multispectral, multiangular and polarimetric measurements over ocean, *Atmospheric Measurement Techniques*, 9, 2877–2907, 2016.

Xu, F., van Harten, G., Diner, D. J., Kalashnikova, O. V., Seidel, F. C., Bruegge, C. J., and Dubovik, O.: Coupled retrieval of aerosol properties and land surface reflection using the Airborne Multiangle SpectroPolarimetric Imager, *Journal of Geophysical Research: Atmospheres*, 122, 7004–7026, <https://doi.org/10.1002/2017JD026776>, <https://agupubs.onlinelibrary.wiley.com/doi/abs/10.1002/2017JD026776>, 2017.

15 Xu, F., Diner, D. J., Dubovik, O., and Schechner, Y.: A Correlated Multi-Pixel Inversion Approach for Aerosol Remote Sensing, *Remote Sensing*, 11, <https://doi.org/10.3390/rs11070746>, <https://www.mdpi.com/2072-4292/11/7/746>, 2019.

Xu, X. and Wang, J.: Retrieval of aerosol microphysical properties from AERONET photopolarimetric measurements: 1. Information content analysis, *Journal of Geophysical Research: Atmospheres*, 120, 7059–7078, <https://doi.org/10.1002/2015JD023108>, <https://agupubs.onlinelibrary.wiley.com/doi/abs/10.1002/2015JD023108>, 2015.

20 Xu, X., Wang, J., Zeng, J., Spurr, R., Liu, X., Dubovik, O., Li, L., Li, Z., Mishchenko, M. I., Siniuk, A., and Holben, B. N.: Retrieval of aerosol microphysical properties from AERONET photopolarimetric measurements: 2. A new research algorithm and case demonstration, *Journal of Geophysical Research: Atmospheres*, 120, 7079–7098, <https://doi.org/10.1002/2015JD023113>, <https://agupubs.onlinelibrary.wiley.com/doi/abs/10.1002/2015JD023113>, 2015.

Zhai, P.-W., Hu, Y., Trepte, C. R., and Lucker, P. L.: A vector radiative transfer model for coupled atmosphere and ocean systems based on
25 successive order of scattering method, *Optics Express*, 17, 2057–2079, 2009.

Zhai, P.-W., Hu, Y., Chowdhary, J., Trepte, C. R., Lucker, P. L., and Josset, D. B.: A vector radiative transfer model for coupled atmosphere and ocean systems with a rough interface, *Journal of Quantitative Spectroscopy and Radiative Transfer*, 111, 1025–1040, 2010.

Zhai, P.-W., Knobelispiesse, K., Ibrahim, A., Franz, B. A., Hu, Y., Gao, M., and Frouin, R.: Water-leaving contribution to polarized radiation field over ocean, *Optics Express*, 25, A689–A708, <https://doi.org/DOI:https://doi.org/10.1364/OE.25.00A689>, 2017.

30 Zhai, P.-W., Boss, E., Franz, B., Werdell, P. J., and Hu, Y.: Radiative Transfer Modeling of Phytoplankton Fluorescence Quenching Processes, *Remote Sensing*, 10, 1309, <https://doi.org/10.3390/rs10081309>, <http://www.mdpi.com/2072-4292/10/8/1309>, 2018.

Zibordi, G., Mélin, F., Berthon, J.-F., Holben, B., Slutsker, I., Giles, D., D’Alimonte, D., Vandemark, D., Feng, H., Schuster, G., Fabbri, B. E.,
Kaitala, S., and Seppälä, J.: AERONET-OC: A Network for the Validation of Ocean Color Primary Products, *Journal of Atmospheric and Oceanic Technology*, 26, 1634–1651, <https://doi.org/10.1175/2009JTECHO654.1>, <https://doi.org/10.1175/2009JTECHO654.1>, 2009.